the plant journal

SEB Society for Experimental Biology

The Plant Journal (2018) **93,** 34–49 doi: 10.1111/tpj.13755

Non-branched β-1,3-glucan oligosaccharides trigger immune responses in Arabidopsis

Hugo Mélida[1], Sara Sopeña-Torres[1], Laura Bacete[1,2], María Garrido-Arandia[1], Lucía Jordá[1,2], Gemma López[1], Antonio Muñoz-Barrios[1,2], Luis F. Pacios[1,3] and Antonio Molina[1,2,*]

[1]*Centro de Biotecnología y Genómica de Plantas, Universidad Politécnica de Madrid (UPM) – Instituto Nacional de Investigación y Tecnología Agraria y Alimentaria (INIA), Campus de Montegancedo UPM, 28223 Pozuelo de Alarcón (Madrid), Spain,*

[2]*Departamento de Biotecnología-Biología Vegetal, Escuela Técnica Superior de Ingeniería Agronómica, Alimentaría y de Biosistemas, UPM, 28040 Madrid, Spain, and*

[3]*Departamento de Sistemas y Recursos Naturales, Escuela Técnica Superior de Ingeniería de Montes, UPM, 28040 Madrid, Spain*

Received 6 July 2017; revised 5 September 2017; accepted 13 October 2017; published online 30 October 2017.
*For correspondence (e-mail antonio.molina@upm.es).

SUMMARY

Fungal cell walls, which are essential for environmental adaptation and host colonization by the fungus, have been evolutionarily selected by plants and animals as a source of microbe-associated molecular patterns (MAMPs) that, upon recognition by host pattern recognition receptors (PRRs), trigger immune responses conferring disease resistance. Chito-oligosaccharides [β-1,4-*N*-acetylglucosamine oligomers, $(GlcNAc)_n$] are the only glycosidic structures from fungal walls that have been well-demonstrated to function as MAMPs in plants. Perception of $(GlcNAc)_{4–8}$ by Arabidopsis involves CERK1, LYK4 and LYK5, three of the eight members of the LysM PRR family. We found that a glucan-enriched wall fraction from the pathogenic fungus *Plectosphaerella cucumerina* which was devoid of GlcNAc activated immune responses in Arabidopsis wild-type plants but not in the *cerk1* mutant. Using this differential response, we identified the non-branched 1,3-β-D-(Glc) hexasaccharide as a major fungal MAMP. Recognition of 1,3-β-D-$(Glc)_6$ was impaired in *cerk1* but not in mutants defective in either each of the LysM PRR family members or in the PRR-co-receptor BAK1. Transcriptomic analyses of Arabidopsis plants treated with 1,3-β-D-$(Glc)_6$ further demonstrated that this fungal MAMP triggers the expression of immunity-associated genes. *In silico* docking analyses with molecular mechanics and solvation energy calculations corroborated that CERK1 can bind 1,3-β-D-$(Glc)_6$ at effective concentrations similar to those of $(GlcNAc)_4$. These data support that plants, like animals, have selected as MAMPs the linear 1,3-β-D-glucans present in the walls of fungi and oomycetes. Our data also suggest that CERK1 functions as an immune co-receptor for linear 1,3-β-D-glucans in a similar way to its proposed function in the recognition of fungal chito-oligosaccharides and bacterial peptidoglycan MAMPs.

Keywords: necrotrophic fungi, plant immunity, cell wall, glucan, chitin, CERK, BAK1.

INTRODUCTION

Fungi and oomycetes are major plant pathogens that cause devastating diseases in crops (Fisher *et al.*, 2012). Immune responses in plants can be triggered by microbe-associated molecular patterns (MAMPs) upon extracellular perception by pattern recognition receptors (PRRs) resident in the plasma membrane; these receptors activate so-called pattern-triggered immunity (PTI). These PTI responses mediated by receptors feed into calcium-dependent and mitogen-activated protein kinase (MAPK) signalling cascades. The latter comprise three types of kinases [MAP kinase kinase kinases (MAP3Ks/MEKKs), MAP kinase kinases (MAPKKs/MKKs) and MAP kinases (MAPKs/MPKs)] which are highly conserved in eukaryotes and play pivotal roles in the activation of transcriptional immune responses and upregulation of specific defensive genes (Bigeard *et al.*, 2015).

Immune responses and disease resistance to pathogens are compromised in plants defective in PRRs perceiving

© 2017 The Authors
The Plant Journal © 2017 John Wiley & Sons Ltd

microbial MAMPs such as FLS2 (flagellin sensing 2), a receptor like kinase (RLK) with a leucine-rich-repeat (LRR) ectodomain (LRR-RLK) which recognizes the bacterial flg22 peptidic MAMP (Gómez-Gómez and Boller, 2000). The activity of PRRs of the LRR-RLK group depends mainly on co-receptors of the SERK (somatic embryogenesis receptor kinase) family, which are also involved in developmental processes and initiation of cell death (Kemmerling *et al.*, 2007; Li, 2010). BAK1/SERK3 [brassinosteroid insensitive 1 (BRI1) associated kinase 1] hetero-oligomerizes with FLS2 and other LRR-RLKs upon recognition of MAMPs, forming dynamic complexes. Based on its multiple interactions, BAK1 has been suggested to be a co-receptor in plasma membrane-associated protein complexes comprising LRR-RLKs, but also some LRR-receptor like proteins (RLPs) that are required for fungal resistance (Zhang *et al.*, 2013; Albert *et al.*, 2015).

Plants and animals have evolutionarily selected fungal cell walls as a source of MAMPs. Fungal cell wall is a semi-rigid and dynamic structure composed primarily of polysaccharides, like chitin and glucans, and highly glycosylated proteins (Latgé and Calderone, 2006). During the initial steps of host–fungus interaction in the extracellular spaces of plant tissues, host-derived toxins and hydrolytic enzymes, such as chitinases and glucanases, target the integrity of the fungal cell wall, and wall fragments that function as MAMPs are released, activating host immune responses (Rovenich *et al.*, 2016). Fungal chitin, a linear polymer of β-1,4-linked *N*-acetylglucosamine (GlcNAc) residues, has been demonstrated to function as a MAMP in plants (Kaku *et al.*, 2006). Chitin is present throughout the whole fungal kingdom and can be considered as the main criterion for identification of fungal cell walls; plants and bacteria are devoid of chitin. In Arabidopsis, lysine motif-(LysM)-RLK CERK1 (chitin elicitor receptor kinase 1) plays a central role in chitin-triggered immune signalling (Miya *et al.*, 2007; Wan *et al.*, 2008). AtCERK1 was initially reported to directly bind chitin oligosaccharides, although with a low affinity (Liu *et al.*, 2012). Also, the LysM PRR family members AtLYK4 and LYK5 have been shown to bind chitin oligosaccharides with much higher affinity than CERK1 (Cao *et al.*, 2014). However, LYK4 and LYK5 lack an active kinase domain, and thus the formation of heterodimeric complexes such as LYK4/5-CERK1 has been suggested (Cao *et al.*, 2014). More recently it has been suggested that CERK1, in addition to activating downstream components of the chitin signalling cascade through phosphorylation events, phosphorylates LYK5, inducing its sequestration into endosomes, while CERK1 itself stays at the plasma membrane (Erwig *et al.*, 2017). Removal of LYK5 from the chitin receptor complex would facilitate the assembly of signalling-competent receptor complexes with newly synthesized LYK5 or other complex components (Erwig *et al.*, 2017).

AtCERK1 is also involved in the recognition of the bacterial peptidoglycan glycosidic moiety in another heteromeric complex with the LysM receptors LYM1 and LYM3 (Willmann *et al.*, 2011). It is worth highlighting that although the glycosidic ligand does not bind to CERK1 directly, all three proteins in the heteromeric complex are required for the activation of peptidoglycan-inducible defences and immunity to bacterial infection. Thus, CERK1, analogously to BAK1, seems to act as a co-receptor in plasma membrane complexes transducing glycan-based MAMP signals in collaboration with receptors having higher specificity.

Glucans represent another family of wall polymers that are widely distributed across the fungal kingdom, which include mainly structures with β-1,3 and β-1,6 linkages, although α-1,3- and α-1,4-linked glucans also occur in some fungal species (Latgé and Calderone, 2006). Glucans are well-known modulators of the immune system in mammals, but despite the higher abundance of glucans in fungal and oomycete cell walls compared with chitin, little is known about the capacity of glucans to trigger PTI in plants (Fesel and Zuccaro, 2016; Rovenich *et al.*, 2016). Pioneering work in the 1970s demonstrated that glucan mixtures from filtrates and mycelial extracts of *Colletotrichum* species were able to induce responses in tomato and bean (Anderson, 1978, 1980). However, the most investigated glucan molecules in the field are the β-1,6-glucan heptaglucosides partially purified from the cell walls of phytopathogenic oomycetes from the orders Pythiales and Peronosporales (Ayers *et al.*, 1976; Ebel *et al.*, 1976; Albersheim and Valent, 1978; Sharp *et al.*, 1984). Later on, Yamaguchi *et al.* (2000) demonstrated that β-1,3-glucan oligosaccharides with at least one β-1,6 branch that were purified from *Magnaporthe oryzae* cell walls induced phytoalexin biosynthesis in suspension-cultured rice cells. Until very recently, it was unclear whether β-glucans are recognized as MAMPs by Arabidopsis ecotypes, thus seriously hampering research in the field (Ménard *et al.*, 2004; Fesel and Zuccaro, 2016; Wawra *et al.*, 2016). In contrast, β-glucans are well-known mammalian MAMPs that are recognized by dectin-1, a *bona fide* β-glucan receptor described in mice and humans (Czop, 1986; Williams, 1997; Ariizumi *et al.*, 2000; Brown and Gordon, 2003). Dectin-1 consists of an extracellular C-type lectin domain that is connected to the plasma membrane by a stalk (Brown *et al.*, 2003). The extracellular lectin domain of dectin-1 binds to β-1,3-glucans and mixed β-1,3/-1,6-glucans, being linear b-1,3-(Glc)10 or a glucan heptasaccharide with one b-1,6-linked glucose side-chain the minimal structures required for binding (Brown *et al.*, 2003; Palma *et al.*, 2006; Adams *et al.*, 2008).

As a first step towards a better understanding of the mechanisms involved in fungal perception by plants and the identification of fungal carbohydrate based-structures

© 2017 The Authors

1365313x, 2018, 1, Downloaded from https://onlinelibrary.wiley.com/doi/10.1111/tpj.13755 by Bucle - Universidad De Leon, Wiley Online Library on [13/05/2024]. See the Terms and Conditions (https://onlinelibrary.wiley.com/terms-and-conditions) on Wiley Online Library for rules of use; OA articles are governed by the applicable Creative Commons License

that activate PTI, we have characterized the cell wall composition of the necrotrophic fungus *Plectosphaerella cucumerina*, a natural pathogen of *Arabidopsis thaliana* (Llorente *et al.*, 2005; Ramos *et al.*, 2013). We obtained several PTI-active wall fractions that were biochemically analysed and tested for their capacity to induce the hallmarks of PTI (e.g. elevated cytoplasmic Ca^{2+}, phosphorylation of MAPKs and upregulation of PTI marker genes). Using this strategy, we identified non-branched β-1,3-glucan oligosaccharides as novel, active MAMPs in Arabidopsis. Moreover, we found that CERK1 is required for the activation of β-1,3-glucan-inducible defence responses and disease resistance to fungal and oomycete infections, further expanding its previously described functions in the perception of chitin and peptidoglycan.

RESULTS

Plectosphaerella cucumerina cell walls are primarily comprising glucans

We studied the cell wall composition of *P. cucumerina*, an ascomycete pathogenic fungus that infects Arabidopsis and other plant species (Llorente *et al.*, 2005; Ramos *et al.*, 2013). Cell wall carbohydrates were purified from mycelial and spore cells by sequential extraction of other cellular components such as lipids, non-covalently bound proteins and glycogen (Figure S1). Carbohydrate analysis of polysaccharides in the mycelial cell wall revealed that they contain glucose (Glc; 61%) and *N*-acetylglucosamine (GlcNAc; 20.4%) as the two most abundant monomers, with lower amounts of galactose (12.3%) and mannose (6.1%) (Figure 1a). This composition was similar to that of the majority of filamentous ascomycete fungi that are typically described as containing β-glucans and chitin [1,4-β-D-$(GlcNAc)_n$] as their main cell wall carbohydrates (Latgé and Calderone, 2006). Glycosidic linkage analysis showed that a large proportion of the glucosyl residues in the mycelial cell walls of *P. cucumerina* arises from 1,3-glucans with a rather low proportion of residues indicative of 1,6-branching points (e.g. 1,3,6-Glc in Figure S2). Most of the mycelial glucan polysaccharides were readily hydrolysable by trifluoroacetic acid (TFA) (89%; TFA-soluble), which indicates low supramolecular complexity or a low crystallinity index. By contrast, almost 90% of the monomeric constituents of wall chitin were not hydrolysed and solubilized by TFA (TFA-insoluble fraction) and were only released after strong sulphuric hydrolysis, indicating that chitin was in a highly crystalline polymeric structure in the wall of the mycelium (Figure 1a). Methylation of these chitin polymers prior to hydrolysis showed that the GlcNAc fraction was dominated by 1,4-linked residues (about 99.9%) together with minute amounts of terminal non-reducing sugars (Figure S2), pointing to the occurrence of chitin chains having a high degree of polymerization (dp). In addition to glucans and chitin, *P. cucumerina* mycelial walls also contain other heteropolysaccharides, accounting for 18.6% of its molar composition (Figure 1a). Our data clearly demonstrate the presence of complex heteromannan–galactofuronan polymers in the cell wall of this necrotrophic fungus which also occur in other ascomycetes (Figure S2) (Leal *et al.*, 2010).

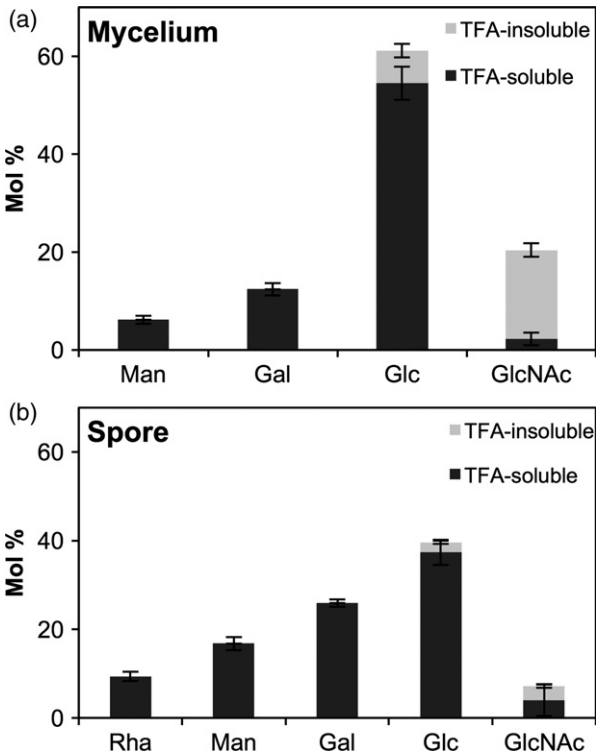

Figure 1. Monosaccharide composition (mol%) of the total cell walls from *Plectosphaerella cucumerina*.
(a) Mycelium.
(b) Spores.
Monosaccharides from purified cell walls were released in a two-step hydrolysis procedure: first with trifluoroacetic acid (TFA; TFA-soluble) and in a second instance the remaining TFA-insoluble polysaccharides were fully hydrolysed with sulphuric acid. Values are means ± SD, $n = 6$. Rha, rhamnose; Man, mannose; Gal, galactose; Glc, glucose; GlcNAc, *N*-acetylglucosamine.

Most of the efforts to characterize fungal cell walls have been typically focused on mycelial walls and currently there is little information about spore wall composition. We determined *P. cucumerina* spore cell wall composition and found that it resembles the mycelial composition, but clear differences can be observed after a detailed analysis (Figure 1b). Although present in lower amounts, glucose was still the main component (39.5%) and only 5% of the glucan-containing polysaccharides remained resistant to TFA hydrolysis (TFA-insoluble; Figure 1b). The amount of GlcNAc was reduced in the cell wall of the spores, and was actually the least abundant component (7%) of the five monosaccharides found in measurable amounts.

© 2017 The Authors

1365313x, 2018, 1, Downloaded from https://onlinelibrary.wiley.com/doi/10.1111/tpj.13755 by Bucle - Universidad De Leon, Wiley Online Library on [13/05/2024]. See the Terms and Conditions (https://onlinelibrary.wiley.com/terms-and-conditions) on Wiley Online Library for rules of use; OA articles are governed by the applicable Creative Commons License

Moreover, its structure must be different from the mycelial polymer, since more than 50% of chitin polymer in the spore counterpart was soluble after TFA hydrolysis (Figure 1b). On the other hand, galactose (25.9%) and mannose (16.8%) became the second and third most abundant monosaccharides in spore walls, and rhamnose was also present (9.4%), in contrast to mycelial walls. Together these data indicate that the spore walls have a different structure with a stronger contribution from mannan–galactofuronan heteropolymers.

Carbohydrate-enriched mycelial wall fractions contain MAMPs

Upon perception of a MAMP by its counterpart PRR an early cytoplasmic Ca^{2+} influx (burst) occurs with subsequent activation of downstream signalling networks (Ranf *et al.*, 2011; Seybold *et al.*, 2014). This early immune Ca^{2+} burst can be detected in Arabidopsis transgenic lines expressing the aequorin Ca^{2+} sensor (Col-0^{AEQ}) upon treatment of the plant with pure MAMPs (Ranf *et al.*, 2011, 2012) such as chitin (Merck KGaA, Darmstadt, Germany) or different *P. cucumerina* cell wall fractions (purified in this work) (Figure 2). Both mycelial and spore cell walls from *P. cucumerina* induce a slight Ca^{2+} influx in their crude (non-fractionated; AIR) forms, similarly to crude freeze-dried cells not subjected to any purification (Myc and Spore prep), or the long linear β-1,3-glucan polysaccharide (curdlan, Megazyme, Wicklow, Ireland) used as a standard (Figure 2a, b). Several PTI active wall fractions were obtained from mycelia and spores of *P. cucumerina* upon treatment with hot methanol–KOH solutions (Figure S1). According to the intensity of the Ca^{2+}-associated burst induced after incubation with these active alkali soluble fractions (ASF), we selected mycelial fractions as better candidates than spore ones for the identification of novel fungal MAMPs.

Interestingly, carbohydrate analysis of selected *P. cucumerina* cell wall fractions showed that the most active wall fraction (ASF-II) was devoid of chitin but contained 60% Glc, whereas AIF was dominated by glucans and

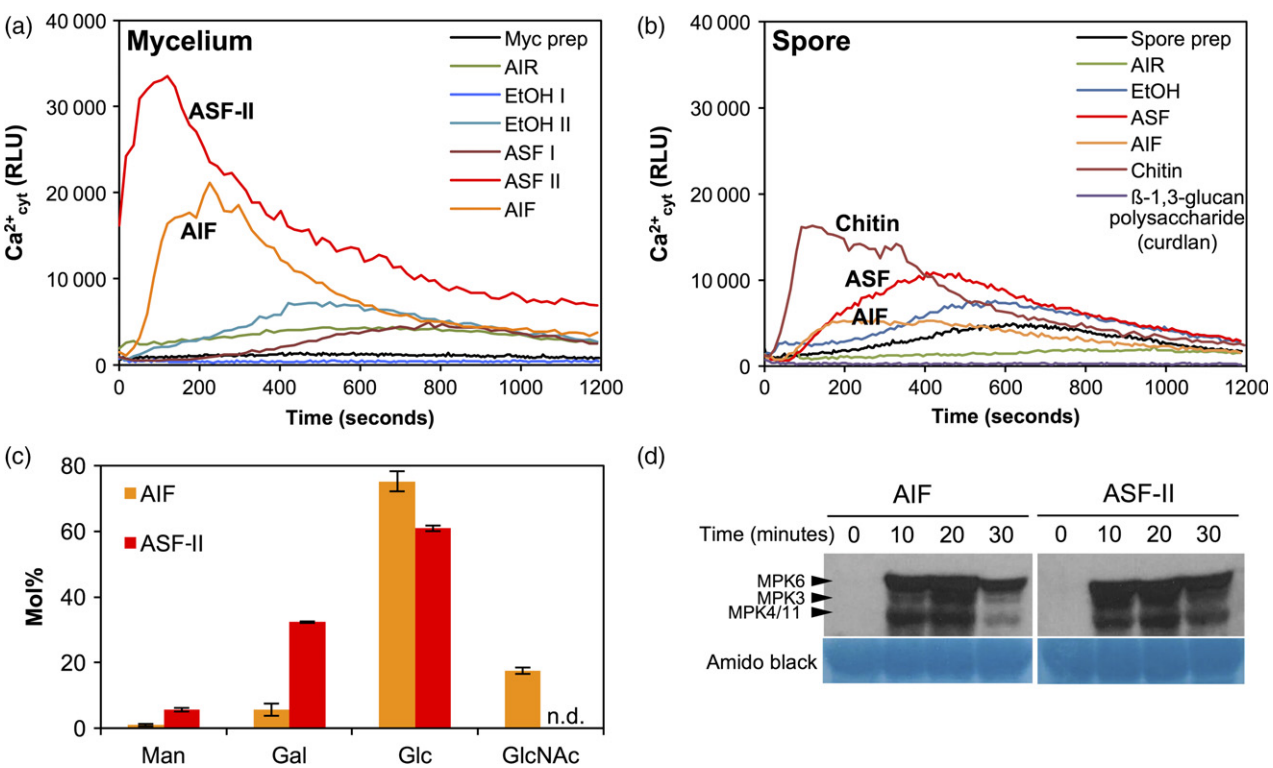

Figure 2. *Plectosphaerella cucumerina* carbohydrate-enriched wall fractions contain microbe-associated molecular patterns (MAMPs).
Elevations of cytoplasmic calcium concentrations over time in Arabidopsis Col-0^{AEQ} seedlings upon treatment with different *P. cucumerina* mycelial (a) and spore (b) cell wall extracts and commercial standards (0.5 μg μl^{-1}) measured as relative luminescence units (RLU). Freeze-dried cell preparations (Myc prep and Spore prep), alcohol insoluble residues (AIR), ethanol-soluble extracts (EtOH-I and -II), alkali-soluble fractions I and II (ASF-I and -II) and the alkali insoluble fraction (AIF) were tested in Col-0^{AEQ} seedlings. Data are representative of three independent experiments with similar results (means, $n = 8$).
(c) Monosaccharide composition (mol%) of ASF-II and AIF was determined by GC-MS. Values are means ± SD, $n = 6$. Man, mannose; Gal, galactose; Glc, glucose; GlcNAc, *N*-acetylglucosamine; n.d., not detected.
(d) Mitogen-activated protein kinase phosphorylation upon application of ASF-II and AIF fractions containing wall MAMPs (0.5 μg μl^{-1}). The phosphorylation of MPK6, MPK3 and MPK4/MPK11 was determined by Western blot, using the anti-pTEpY antibody, at the indicated time points (min) upon treatment. Amido black-stained membranes show equal loading. Data are representative of three independent experiments.

© 2017 The Authors

1365313x, 2018, 1, Downloaded from https://onlinelibrary.wiley.com/doi/10.1111/tpj.13755 by Bucle - Universidad De Leon, Wiley Online Library on [13/05/2024]. See the Terms and Conditions (https://onlinelibrary.wiley.com/terms-and-conditions) on Wiley Online Library for rules of use; OA articles are governed by the applicable Creative Commons License

contained a reasonable amount of chitin (17.5%) (Figure 2c). The chitin in AIF must have been partially solubilized (and/or deacetylated) with the hot alkali treatments used to obtain it, and therefore might be readily perceived by PRRs in contrast to crude cell wall preparations (AIR), which despite displaying similar chitin levels produced a noticeably lower increase in cytoplasmic Ca^{2+} levels (Figure 2a, b).

To corroborate the PTI activity of these wall fractions, we next monitored the phosphorylation of downstream kinases (MPK3/MPK6/MPK4/MPK11) upon treatment of Arabidopsis plants with the active AIF and ASF-II wall fractions from *P. cucumerina* mycelium (Figure 2d). Notably, the glucan-enriched, ASF-II fraction devoid of chitin activated MAPK phosphorylation similarly to the chitin-enriched AIF fraction (Figure 2d), suggesting that linear and branched 1,3/1,6-glucans present in ASF-II could operate as MAMPs.

β-1,3 -Glucan oligosaccharides induce CERK1-mediated PTI responses

ASF-II and AIF cell wall fractions were further analysed for their capacity to induce PTI responses on Columbia-0 (Col-0) wild-type plants and in *cerk1-2* and *bak1* mutants (in the Col-0 background) impaired in PRR co-receptors

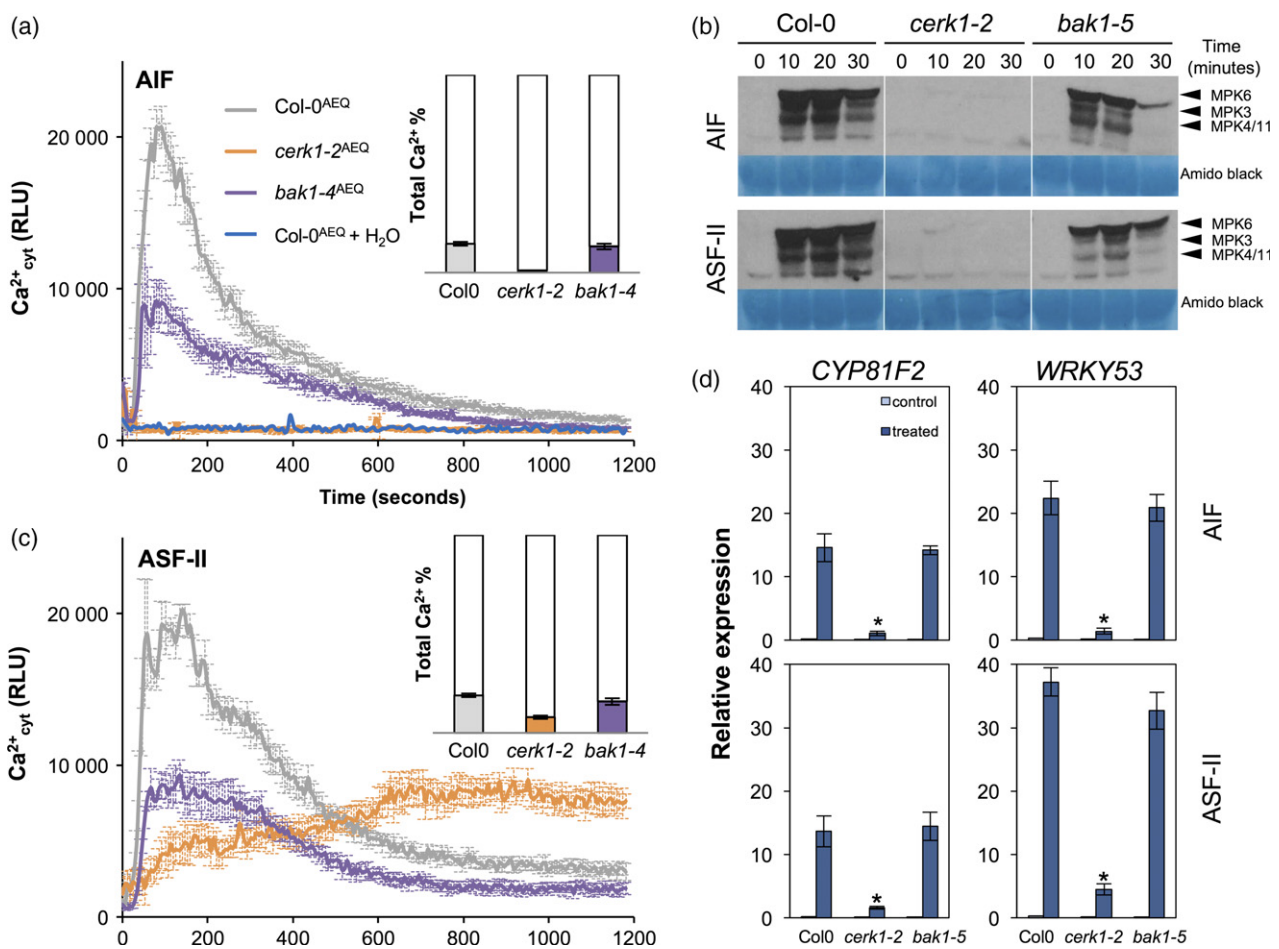

Figure 3. Activation of pattern-triggered immunity responses by *P. cucumerina* AIF and ASF-II microbe-associated molecular patterns (MAMPs) containing fractions is impaired in the *cerk1-2* mutant.

(a), (c) Elevations of cytoplasmic calcium concentrations over time in Arabidopsis Col-0^{AEQ}, *cerk1-2*^{AEQ} and *bak1-4*^{AEQ} seedlings upon treatment (0.25 μg μl^{-1} of fraction) measured as relative luminescence units (RLU). Water (shown in panel a) was used in all the experiments as a negative control. After recording the elicitor-induced Ca^{2+} kinetics, the total calcium was discharged by the addition of $CaCl_2$ to the wells. The kinetic areas after both treatments were integrated and their values used for calculation of the total Ca^{2+}% induced by the treatment compared with the total calcium discharge, which was genotype-dependent.

(b) Mitogen-activated protein kinase activation in 12-day-old Arabidopsis seedlings of the indicated genotypes (0.25 μg μl^{-1} of fraction). The phosphorylation of MPK6, MPK3 and MPK4/MPK11 was determined by Western blot, using the anti-pTEpY antibody, at the indicated time points (min) after treatment. Amido black-stained membranes show equal loading.

(d) Quantitative RT-PCR analyses of defence and MAMP-induced genes in Arabidopsis seedlings of the indicated genotypes after treatment with wall fractions (0.25 μg μl^{-1} for 30 min). Relative expression levels to the *UBC21* (*At5 g25760*) gene are shown. Values are means ± SE, $n = 4$. Asterisks indicate genotypes with significant differences compared with wild-type plants (Col-0) (Student's *t*-test analysis, $*P < 0.05$). In all cases, data are representative from one out of three independent experiments with similar results.

© 2017 The Authors

1365313x, 2018, 1, Downloaded from https://onlinelibrary.wiley.com/doi/10.1111/tpj.13755 by Bucle - Universidad De Leon, Wiley Online Library on [13/05/2024]. See the Terms and Conditions (https://onlinelibrary.wiley.com/terms-and-conditions) on Wiley Online Library for rules of use; OA articles are governed by the applicable Creative Commons License

(Figures 3 and S3). Notably, contrasting with the intense responses observed in Col-0, and *bak1* plants, the *cerk1-2* plants were defective in the perception of AIF and ASF-II fractions since they showed, in comparison with Col-0 plants, a weak or almost null activation of early immune responses such as cytoplasmic Ca^{2+} influxes, phosphorylation of MPK3/MPK6/MPK4/MPK11 or upregulation of PTI-reporter genes (e.g. *CYP81F2*, *WRKY53*, *FRK1*, *PHI-1* and *NHL10*) (Figures 3 and S3).

The clear absence of PTI activation in *cerk1-2* upon treatment with the ASF-II fraction deserved further investigation to unveil the glycosidic nature of the MAMPs responsible for the observed CERK1-dependent immune activation, since this fraction was devoid of chitin (Figure 2c). The main constituents of ASF-II fractions are glucans and, within these, the main type of glycosidic linkages in the *P. cucumerina* cell wall are of type 1,3 (Figure S2). We analysed the purified ASF-II by matrix-assisted laser desorption/ionization time-of-flight tandem mass spectrometry (MALDI-TOF/TOF MS) and found several hexose oligomers (dp = 4–7), the hexamer signals being the more intense ones (Figure S4). Bearing in mind the abundance of 1,3-glucans in *P. cucumerina* cell walls (Figure S2) and the presence of these hexose oligomers in ASF-II (Figure S4), we decided to analyse in the first instance the regulation of PTI by the simplest molecules fulfilling these criteria: short unbranched 1,3-glucans. Pure 1,3-β-D-$(Glc)_6$ (Megazyme) was tested for its capacity to trigger cytoplasmic Ca^{2+} influx, phosphorylation of MPK3/MPK6/MPK4/MPK11 and upregulation of PTI-reporter genes (*CYP81F2*, *WRKY53*, *FRK1*, *PHI-1* and *NHL10*) on Col-0, *cerk1-2* and *bak1* lines (Figures 4 and S5). The 1,4-β-D-$(GlcNAc)_6$ oligosaccharide (Megazyme) and the bacterial MAMP flg22 (EZBiolab) were included as controls in most of these experiments (Col-0 background lines). These analyses confirmed that linear 1,3-β-D-$(Glc)_6$, was recognized by Arabidopsis plants and that this recognition was independent of BAK1 and, remarkably, dependent on CERK1 (Figures 4 and S5), as it occurs with chito-oligosaccharide and peptidoglycan perception (Willmann *et al.*, 2011; Liu *et al.*, 2012). To further corroborate this novel CERK1 function, we tested the responses to 1,3-β-D-$(Glc)_6$ and 1,4-β-D-$(GlcNAc)_6$ oligosaccharides (Megazyme) of *cerk1-3* plants, an additional mutant allele in the Ws-4 background. In these experiments we used the damage-associated molecular patterns (DAMPs) oligogalacturonides [OGs (1,4-α-D-$(GalA)_{10–15}$, Elicityl); Nothnagel *et al.*, 1983) as positive controls, since some Ws ecotypes do not perceive flg22 (Gómez-Gómez *et al.*, 1999). As shown in Figure S6 *cerk1-3* plants were also defective in MAPK phosphorylation and activation of PTI gene expression upon treatment with 1,3-β-D-$(Glc)_6$ and 1,4-β-D-$(GlcNAc)_6$, whereas these PTI hallmarks were similar in *cerk1-3* and Ws-4 plants treated with 1,4-α-D-$(GalA)_{10–15}$. Activation of the reactive oxygen species (ROS) production machinery upon 1,3-β-D-$(Glc)_6$ treatment was studied by mean of *in vivo* quantification of the transcriptional regulation of the *RbohD* gene, encoding the NADPH-oxidase RBOHD protein (Morales *et al.*, 2016). *RbohD*-promoter driven luciferase transgenic lines (*pRbohD::LUC*) confirmed the transcriptional activation *RbohD* by the glucan hexasaccharide (Megazyme), but to a much lower extent than flg22 (Figure S7). Such lower transcriptional activation might explain the fact that ROS production in response to this glucan oligosaccharide was not readily measurable in the Arabidopsis Col-0 ecotype using luminol-based methodologies (Figure S7), which contrasts with Ws ecotypes (Wawra *et al.*, 2016).

The glucan hexasaccharide preparation used in our experiments is certified to be of high purity (> 95%; Megazyme) as further demonstrated by MALDI-TOF/TOF MS analyses that we performed (Figure S8a). However, in order to exclude undesired contamination by GlcNAc of the glucan samples [1,3-β-D-$(Glc)_6$ and 1,3-β-D-$(Glc)_{7-16}$ purified by Megazyme (see Figure S11)] employed in our experiments, we performed additional chemical analysis of their composition. As shown in Figure S8(b), these analyses corroborated that the glucan samples do not contain amino sugars (e.g. GlcNAc) in contrast to 1,4-β-D-$(GlcNAc)_6$ and peptidoglycan (Sigma-Aldrich) used in the analysis for comparison.

In order to assess whether other LysM-RLKs might be also involved in the perception of 1,3-β-D-$(Glc)_6$, MAPK phosphorylation was monitored in single mutants of all Arabidopsis LysM-containing proteins (CERK1, LYK2–LYK5, LYM1–LYM3). These analyses demonstrated that only CERK1 was absolutely required for the downstream phosphorylation of MAPKs mediated by the 1,3-glucan hexasaccharide (Figure S9).

CERK1-mediated PTI responses to non-branched β-1,3-glucan are tightly dependent on the degree of polymerization of the glucan

To further investigate whether other β-1,3-glucans than the linear hexasaccharide could trigger PTI responses in Arabidopsis, we tested the capability of different oligo/polysaccharides as well as the D-glucose monomer to induce elevations in cytoplasmic Ca^{2+}. The 1,3-β-D-$(Glc)_5$ oligosaccharide was the smallest one activating PTI (e.g. causing an increase in Ca^{2+}; Figure S10) in a CERK1-dependent manner, whereas the 1,3-β-D-(Glc) tetrasaccharide was not able to activate a Ca^{2+} burst in any of the aequorin lines tested (Figure S10). Interestingly, Ca^{2+} elevations were recovered when the trisaccharide was tested in the Col-0^{AEQ} lines, but these signals might be mediated by an alternative pathway since this response was similarly observed in *cerk1-2*^{AEQ} lines, indicating CERK1 independence (Figure S10). Ca^{2+} elevations were not due to osmotic stress, since we did not observe any response in Col-0^{AEQ} lines treated with D-glucose (Figure S10).

© 2017 The Authors

1365313x, 2018, 1, Downloaded from https://onlinelibrary.wiley.com/doi/10.1111/tpj.13755 by Bucle - Universidad De Leon, Wiley Online Library on [13/05/2024]. See the Terms and Conditions (https://onlinelibrary.wiley.com/terms-and-conditions) on Wiley Online Library for rules of use; OA articles are governed by the applicable Creative Commons License

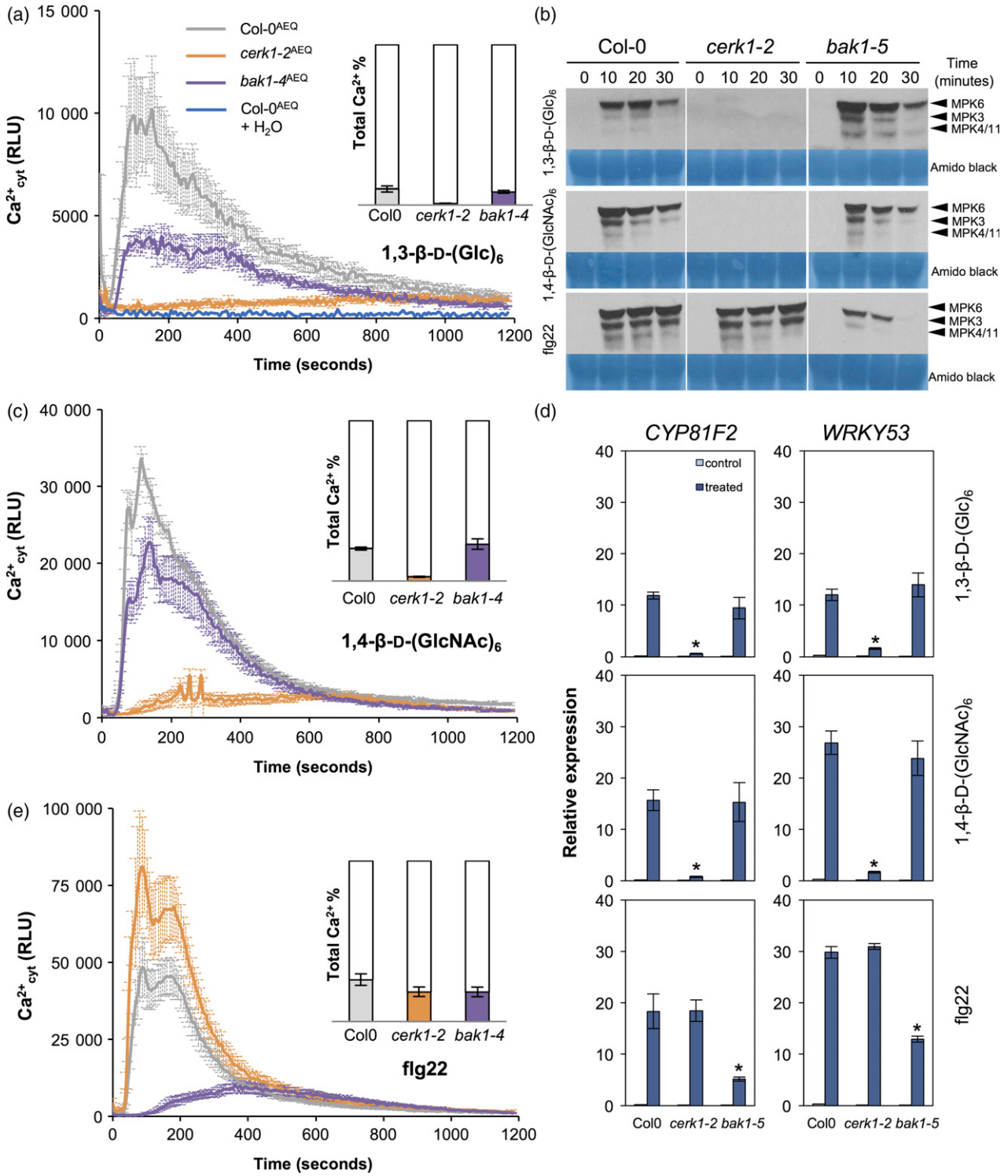

Figure 4. Activation of pattern-triggered immunity responses by 1,3-β-D-(Glc)$_6$, 1,4-β-D-(GlcNAc)$_6$ and flg22.
(a), (c), (e) Elevations of cytoplasmic calcium concentrations over time in Arabidopsis Col-0^{AEQ}, *cerk1-2*^{AEQ} and *bak1-4*^{AEQ} seedlings upon treatments. Water-treated plants, shown in panel (a), were used as a negative control.
(b) Mitogen-activated protein kinase activation and (d) qRT-PCR analyses of defence and microbe-associated molecular pattern (MAMP)-induced genes in MAMP-treated 12-day-old Arabidopsis seedlings of the indicated genotypes. Oligosaccharides were used at 250 μM and flg22 at 1 μM. Asterisks indicate genotypes with significant differences compared with wild-type plants (Col-0) (Student's *t*-test analysis, $*P < 0.05$). In all cases, data are representative from one out of three independent experiments with similar results. For further details see legend to Figure 3.

© 2017 The Authors

1365313x, 2018, 1, Downloaded from https://onlinelibrary.wiley.com/doi/10.1111/tpj.13755 by Bucle - Universidad De Leon, Wiley Online Library on [13/05/2024]. See the Terms and Conditions (https://onlinelibrary.wiley.com/terms-and-conditions) on Wiley Online Library for rules of use; OA articles are governed by the applicable Creative Commons License

In an attempt to determine whether 1,3-β-glucans of dp higher than 6 would trigger similar responses to the hexasaccharide, we tested a mixture of linear 1,3-β-glucans with dp ranging from 7 to 16 purified 'ad hoc' (Megazyme) (Figure S11), which activated an intense PTI on Col-0 but not in *cerk1-2* (Figure S12). In contrast, a highly insoluble non-branched β-1,3-glucan (curdlan, Megazyme) lacked PTI-activity, indicating that insoluble polymers must first be processed to soluble entities to be recognized as MAMPs (Figure S13). Remarkably, the soluble laminarin polymer (β-1,3-glucan 1,6-branched, Thermo Fisher) activated a slight Ca^{2+} influx that was independent of CERK (Figure S13). This result indicates that either crude laminarin preparations contain impurities that are able to trigger such influxes of Ca^{2+} or that different β-glucan structures trigger PTI responses through distinct PRR complexes.

Comparative mechanisms between β-1,3-glucan-oligosaccharides and chito-oligosaccharides

To further characterize the kinetics of perception of 1,3-β-D-$(Glc)_6$ by Arabidopsis, we performed dose–response studies using Col-0^{AEQ} lines (Figure 5a). The results indicated that the glycosidic MAMPs 1,3-β-D-$(Glc)_6$ and 1,4-β-D-$(GlcNAc)_6$ showed estimated effective doses (EED; 50% of total signal) in the micromolar range, although they have different kinetics. We performed similar dose–response analyses with Col-0^{AEQ} using flg22 and obtained a clear sigmoid kinetic with an EED of 10.55 nM, a concentration that was in the same range as the affinity FLS2-flg22 values estimated using other methods (Bauer *et al.*, 2001; Chinchilla *et al.*, 2006) (Figure S14).

In silico docking analyses were performed using the structure of the Arabidopsis CERK1-ectodomain (AtCERK1-ECD) to computationally determine if CERK1 could bind 1,3-β-D-$(Glc)_6$, in addition to the described 1,4-β-D-$(GlcNAc)_4$ (Liu *et al.*, 2012, 2016). AtCERK1-ECD–1,4-β-D-$(GlcNAc)_6$ complexes optimized from initial docking geometries reveal that the orientation of the 1,4-β-D-$(GlcNAc)_6$ oligosaccharide is nearly coincident with that corresponding to the 1,4-β-D-$(GlcNAc)_4$ ligand present in the 4EBZ crystal structure of AtCERK1-ECD, further supporting our *in silico* analyses (Figure 5b). We found that CERK1 could bind 1,3-β-D-$(Glc)_6$, but clear differences in orientation were noticed in the AtCERK1-ECD-1,3-β-D-$(Glc)_6$ structure compared with that of AtCERK1-ECD–1,4-β-D-$(GlcNAc)_6$ (Figure 5b). However, these structural differences between 1,4-β-D-$(GlcNAc)_6$ and 1,3-β-D-$(Glc)_6$ were not reflected in the protein–ligand affinity energies ΔG_{aff} estimated from the docking procedure (Table S1). Then, we determined the protein–glycan interaction energies (see Experimental procedures), and in these optimized structures we found essential differences (Table S1): the AtCERK1–1,4-β-D-$(GlcNAc)_6$ complex had lower protein–glycan attractive energies ($\Delta E_{elec} + \Delta E_{vdW}$) than the AtCERK1–1,3-β-D-$(Glc)_6$ complex, particularly the van der Waals interactions which are about −45 kcal mol^{-1} in β-1,4 systems and about −24 kcal mol^{-1} in β-1,3 systems. Altogether these *in silico* data predict that 1,3-β-D-$(Glc)_6$, as the chitin hexamer, might bind to AtCERK1. However, given previous data pointing to the role of CERK1 as a PRR co-receptor, it can be hypothesized that additional PRRs would bind, with higher affinity, the 1,3-β-D-$(Glc)_6$ ligand and will present it

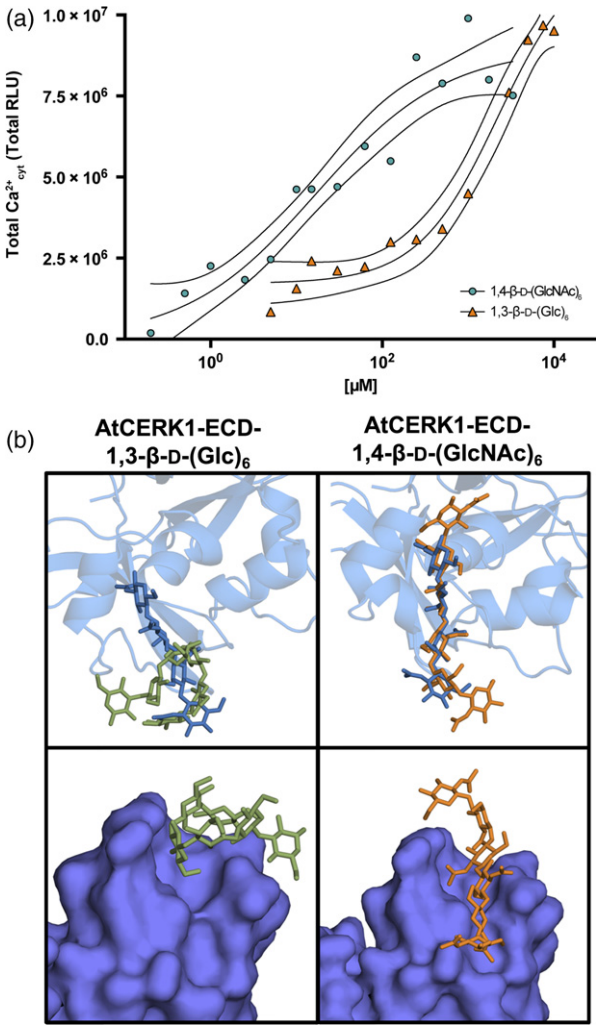

Figure 5. Comparative kinetics responses and binding to CERK1 of 1,3-β-D-$(Glc)_6$ and 1,4-β-D-$(GlcNAc)_6$ microbe-associated molecular patterns (MAMPs).

(a) Dose–response, determined as increase in total cytoplasmic calcium, was measured in Arabidopsis Col-0^{AEQ} seedlings treated with increasing concentrations of 1,3-β-D-$(Glc)_6$ or 1,4-β-D-$(GlcNAc)_6$. Values are averages of at least eight replicates. Calcium saturation curves were adjusted using Prism 6 Software, and the dashed curves represent the 95% confidence intervals.

(b) Binding site in the optimized structures of AtCERK1-ECD–1,3-β-D-$(Glc)_n$ and AtCERK1-ECD–1,4-β-D-$(GlcNAc)_n$ complexes. Glycans are represented as sticks in green hues for β-1,3 glucans and orange hues for β-1,4 chito-oligosaccharides. Sticks in blue indicate the 1,4-β-D-$(GlcNAc)_4$ ligand present in the crystal structure of its complex with AtCERK1 (PDB ID 4EBZ).

© 2017 The Authors

1365313x, 2018, 1, Downloaded from https://onlinelibrary.wiley.com/doi/10.1111/tpj.13755 by Bucle - Universidad De Leon, Wiley Online Library on [13/05/2024]. See the Terms and Conditions (https://onlinelibrary.wiley.com/terms-and-conditions) on Wiley Online Library for rules of use; OA articles are governed by the applicable Creative Commons License

to CERK1 to further activate the recognition complex (Cao *et al.*, 2014).

Global suite of differentially regulated genes after 1,3-β-D-(Glc)$_6$ elicitor treatment

To further characterize the transcriptional responses regulated by 1,3-β-glucan-MAMPs, we performed RNA sequencing (RNA-seq) analyses of Col-0 and *cerk1-2* seedlings treated for 30 min with pure 1,3-β-D-(Glc)$_6$, (Megazyme) or water (mock) (Figures 6 and S15, Tables S2 and S3). The incubation with the glucan induced the misregulation of 1355 genes, most of which (1014) were upregulated (Figure 6a, Table S2). Interestingly, only 292 of the misregulated genes were found in *cerk1-2*, with 159 being exclusively altered in the *cerk1-2* plants, indicating that the expression of the majority of these 1,3-β-D-(Glc)$_6$ misregulated genes is dependent on CERK1 (Figure 6a). The genes regulated in Col-0 by glucan treatment were mainly grouped into Gene Ontology (GO) terms related to response to different stimuli, including biotic and abiotic stresses and phytohormones, and to transcriptional regulation and protein phosphorylation (Figure 6b, Table S3). Genes exclusively altered in *cerk1-2* were mainly related to abiotic stress responses (Figure S15a, Table S3).

CERK1 is required for plant immunity towards fungal and oomycete infections

CERK1 has been described to contribute to the resistance of Arabidopsis to fungi like *Alternaria brassicicola* and *Erysiphe cichoracearum* (Wan *et al.*, 2008) since the *cerk1* mutant shows enhanced susceptibility to these pathogens. We tested the contribution of CERK1 to additional disease resistance responses to fungi and we first analysed the susceptibility of *cerk1-2* mutant plants to *P. cucumerina*. Three-week-old wild-type (Col-0) and *cerk1-2* plants, and the *agb1-2* and *irx1-6* mutants included as hypersusceptible and resistant controls, respectively (Llorente *et al.*, 2005; Hernández-Blanco *et al.*, 2007), were inoculated with a spore suspension of the fungus. The progression of the infection was determined by macroscopic evaluation of disease rating at different days post-inoculation (dpi) and biomass quantification of *P. cucumerina* by quantitative PCR (qPCR) (at 3 and 5 dpi). As shown in Figure 7(a), biomass quantification indicated that *cerk1-2* plants were more susceptible than wild-type plants to the necrotrophic fungal infection. We have previously demonstrated that ERECTA(ER)-RLK regulates immune responses and resistance to pathogens such as *P. cucumerina* and ER has been suggested to function as a PRR (Llorente *et al.*, 2005; Jordá *et al.*, 2016). Thus, we tested whether the glycosidic MAMPs present in the *P. cucumerina* ASF-II could be recognized by ER. However, this possibility was discarded since MAPK phosphorylation was not altered in *er-105*, *bak1-5* and *er-105 bak1-5* single and double mutants compared with Col-0 plants (Figure S16).

Previous data on oomycete cell wall composition demonstrated that they essentially contain β-1,3-glucan polysaccharides, whereas chitin is absent in the Peronosporales (Mélida *et al.*, 2013). Thus, we tested the resistance of *cerk1-2* plants to the peronosporal oomycete *Hyaloperonospora arabidopsidis*. Col-0 and *cerk1-2* genotypes were inoculated with a conidiospore suspension of

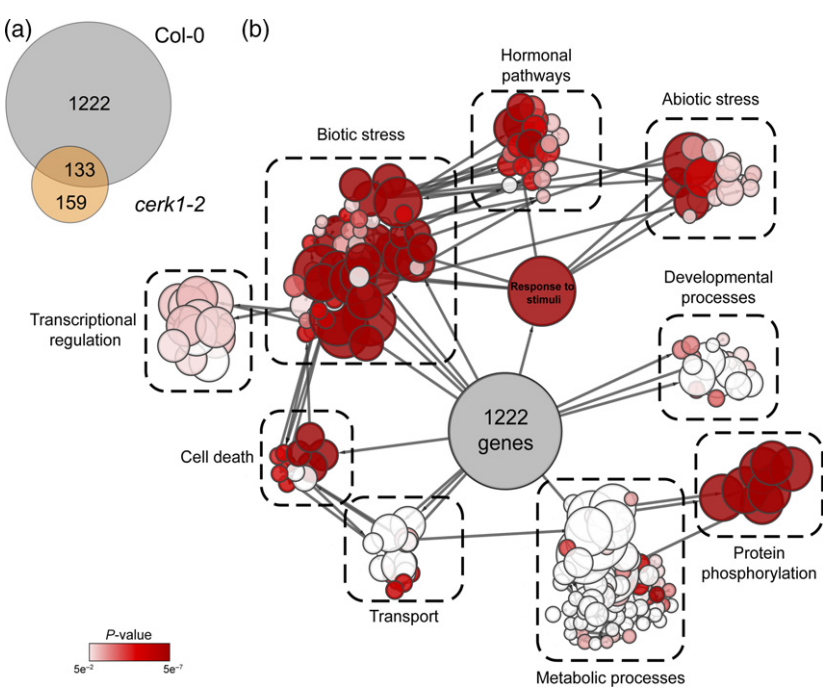

Figure 6. Functional classification of 1,3-β-D-(Glc)$_6$ differentially expressed genes in Arabidopsis.
(a) Venn diagram of shared differentially expressed genes between Col-0 and *cerk1-2* plants treated for 30 min with 250 μM 1,3-β-D-(Glc)$_6$ compared with mock-treated seedlings. See Table S2 for further information on the genes included in each category.
(b) Gene Ontology (GO) biological process-term enrichment network of the 1222 exclusively misregulated genes in Col-0. Each significantly enriched GO term is represented with a circle, the contribution of which (%) is related to its diameter. Significant enrichments were determined using the hypergeometric test and the Benjamini–Hochberg false discovery rate corrected *P*-values are represented using the colour code shown at the bottom right of the figure. As tightly connected GO terms are functionally linked, only the major host responses outputs are indicated (dotted line). See Table S3 for further information on the genes included in each category.

© 2017 The Authors

1365313x, 2018, 1, Downloaded from https://onlinelibrary.wiley.com/doi/10.1111/tpj.13755 by Bucle - Universidad De Leon, Wiley Online Library on [13/05/2024]. See the Terms and Conditions (https://onlinelibrary.wiley.com/terms-and-conditions) on Wiley Online Library for rules of use; OA articles are governed by the applicable Creative Commons License

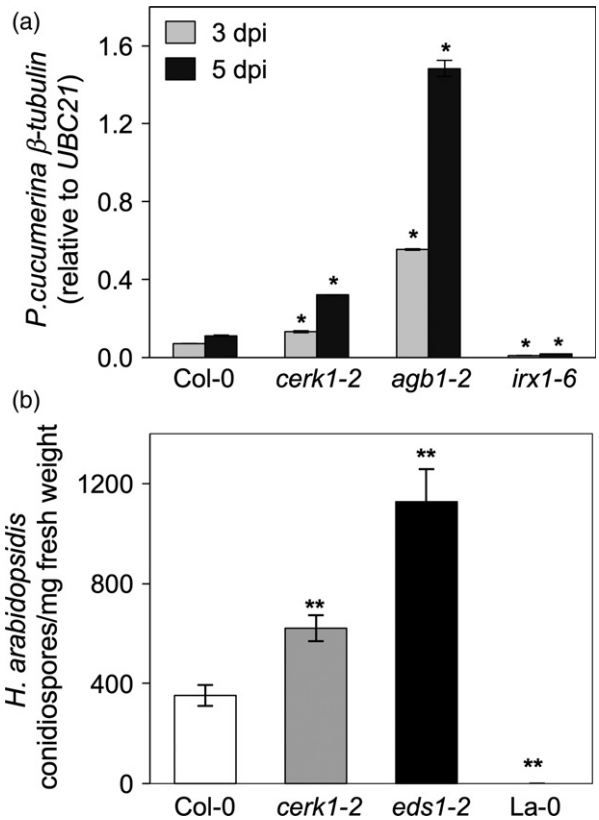

Figure 7. CERK1 is required for resistance of Arabidopsis to necrotrophic and biotrophic pathogens containing glucans in their wall structures.
(a) Resistance of wild-type plants and *cerk1*, *agb1-2* and *irx1-6* mutant plants to the necrotrophic fungus *Plectosphaerella cucumerina* determined by qPCR quantification of fungal biomass (*Pc* β-*tubulin*) at 3 and 5 days post-inoculation (dpi). *agb1-2* and *irx1-6* were included as susceptible and resistant controls, respectively. Data shown are relative expression levels of *Pc* β-*tubulin* to Arabidopsis *UBC21* (*At5 g25760*). Values are means ± SE, $n = 3$. Asterisks indicate genotypes with significant differences in their level of resistance compared with wild-type plants (Col-0) (Student's *t*-test analysis, $*P < 0.05$).
(b) Growth of *Hyaloperonospora arabidopsidis* isolate Noco2 on plants of the indicated genotypes, determined by the production of conidiospores per milligram of leaf fresh weight (FW) at 7 dpi. *eds1-2* and La-0 plants were included as susceptible and resistant controls, respectively. Asterisks indicate genotypes with significant differences in their level of resistance compared with wild-type plants (Col-0) (Student's *t*-test analysis, $**P < 0.01$).

H. arabidopsidis and disease was estimated at 7 dpi in the inoculated plants. The La-0 plants, harbouring the resistance gene for the Noco2 isolate (*RPP5*), and the *eds1* mutant (in La-0 background), defective in effector triggered immunity (ETI) and salicylic acid signalling, were included as susceptible and resistance controls, respectively (Heidrich *et al.*, 2011). Notably, we found that *cerk1-2* plants were more susceptible to this biotrophic oomycete than wild-type plants (Figure 7b). This enhanced growth of the oomycete on *cerk1-2* plants was confirmed by trypan blue staining of the inoculated leaves that revealed enhanced mycelial growth in *cerk1-2* compared with that in Col-0 plants (Figure S17).

DISCUSSION

Cell walls are the first microbe structures to enter into contact with a host in a pathogenic interaction. Fungal cell walls are made up of polysaccharides, some of which are not encountered in plants and animals; thus, these glycosidic structures represent 'non-self', specific targets recognized by the hosts (Geoghegan *et al.*, 2017). These hosts have developed enzymatic machineries that hydrolyse the invader's extracellular polysaccharides, releasing soluble MAMP oligostructures that can reach the outer plasma membrane space where they are ultimately recognized by the ectodomains of host PRRs, triggering immunity (PTI) and activating disease resistance responses (Rovenich *et al.*, 2016). Since this initial recognition of fungal MAMPs makes a significant contribution to onset of host immune response and the effectiveness of disease resistance, a better knowledge of the types of cell wall structures of pathogenic fungi that are recognized by hosts is needed for a rational understanding of plant–pathogen interactions. For this purpose we have performed an in-depth analysis of the cell wall polysaccharide composition of the necrotrophic fungus *P. cucumerina*, a natural pathogen of Arabidopsis (Llorente *et al.*, 2005; Ramos *et al.*, 2013).

Some cell walls within the kingdom Fungi have been biochemically characterized in detail (Latgé and Calderone, 2006; Mélida *et al.*, 2015), but there are few examples of plant-pathogenic fungi whose cell walls have been analysed in detail. Bearing in mind that cell wall composition is known to change under different growth conditions, comparisons are even more difficult unless similar growth conditions and analytical procedures are used. Thus, we collected the *P. cucumerina* mycelium after *in vitro* growth of the fungus in comparable conditions to that used for the characterization of cell wall composition of the necrotroph *B. cinerea* and the hemibiotrophic rice pathogen *Magnaporthe oryzae* (Cantu *et al.*, 2009; Samalova *et al.*, 2017). We found that glucose is the main monosaccharide in the cell wall of *P. cucumerina*, representing 61% of monosaccharides, but the contribution of glucose to wall composition is lower than that in *B. cinerea* and *M. oryzae* walls, where it reaches 90% and 75%, respectively (Cantu *et al.*, 2009; Samalova *et al.*, 2017). On the other hand, the contribution of chitin to wall composition is higher in *P. cucumerina* (GlcNAc represents 20.4% of monosaccharides) than in *B. cinerea* and *M. oryzae* (5 and 7%, respectively; Cantu *et al.*, 2009; Samalova *et al.*, 2017). The contribution of polysaccharides other than glucans and chitin in the *P. cucumerina* cell wall is about 18% (galactose 12.4%, mannose 6.2%), a value similar to that of the hemibiotrophic rice pathogen *M. oryzae* (17%), whereas in the necrotrophic fungus *B. cinerea* the proportion of galactomannans is notably lower (about 5%; Cantu *et al.*, 2009). The characterization of the *P. cucumerina* cell wall

© 2017 The Authors

1365313x, 2018, 1, Downloaded from https://onlinelibrary.wiley.com/doi/10.1111/tpj.13755 by Bucle - Universidad De Leon, Wiley Online Library on [13/05/2024]. See the Terms and Conditions (https://onlinelibrary.wiley.com/terms-and-conditions) on Wiley Online Library for rules of use; OA articles are governed by the applicable Creative Commons License

provided here illustrates the complexity and variability of wall structures of plant pathogens, suggesting that additional mechanisms to those described for chitin recognition might exist in plants to perceive fungal MAMPs derived from cell walls, as occurs in mammals (Latgé, 2017).

Despite of its strong PTI-triggering activity, chitin represents a smaller proportion of the fungal cell walls than do glucans. In the case of *P. cucumerina* mycelial cell walls, the glucan to chitin ratio is 3:1, which is lower than described in other fungi (Latgé and Calderone, 2006). β-Glucans are well characterized MAMPs in fungus–animal systems and their receptors have also been well characterized (Brown and Gordon, 2003). However, the contribution of β-glucans to fungal perception by plants is still poorly understood (Fesel and Zuccaro, 2016). In this work, we have produced *P. cucumerina* wall fractions that are able to activate Arabidopsis PTI responses, such as cytoplasmic Ca^{2+} influxes, MAPK phosphorylation and upregulation of PTI marker genes, in Col-0 wild-type plants but not in the *cerk1* mutant. Using this differential plant response we identified linear 1,3-β-D-(Glc) molecules as fungal MAMPs modulating PTI in Arabidopsis.

The most investigated glucan molecules in the field of plant–pathogen interaction have been the β-1,6-glucan heptaglucosides isolated from the cell walls of phytopathogenic oomycetes from the orders Pythiales and Peronosporales (Ayers *et al.*, 1976; Ebel *et al.*, 1976; Albersheim and Valent, 1978; Sharp *et al.*, 1984). However, β-1,6-glucan backbones have not been reported in fungal walls other than yeasts, and even there they are scarce compared with oomycetes (Latgé and Calderone, 2006). On the other hand, β-1,3-glucans have been clearly understudied. Enzymatically produced β-1,3-glucan pentasaccharides with at least one 1,6-branch induced phytoalexin biosynthesis in suspension-cultured rice cells but not in soybean, which remains intriguing (Yamaguchi *et al.*, 2000). To our knowledge non-branched β-1,3-glucan oligosaccharides had only been reported previously as defence elicitors in tobacco (Klarzynski *et al.*, 2000). Despite these early studies, and recently regained momentum (Wawra *et al.*, 2016), plant-specific knowledge about the mechanisms of β-glucan perception and their role in activation or suppression of defence clearly lags behind the animal field. Our data clearly show that Arabidopsis can perceive non-branched 1,3-β-glucans of various dp and that this recognition is at least partially mediated by CERK1, but it does not involve BAK1, the co-receptor of other PRRs. In line with these molecular data, *in silico* docking analyses indicated that CERK1 would be able to bind 6-mer 1,3-β-glucans, but with clear differences in orientation compared with the binding structure described for chitin (Figure 5b; Liu *et al.*, 2012). Notably, recognition of 1,3-β-D-$(Glc)_6$ was not impaired in mutants defective in Arabidopsis LysM family (LYM1–LYM3 and LYK2–LYK5) members other than CERK1. These data, together with the fact that CERK1 is also required for the perception of MAMP-containing glycan structures such as chitin and bacterial peptidoglycan (Miya *et al.*, 2007; Willmann *et al.*, 2011), suggest that CERK1 might act as a co-receptor, mediating PTI responses induced by several carbohydrate-based MAMPs.

In line with the function of CERK1 in 1,3-β-D-(Glc) perception and PTI activation, we have demonstrated that *cerk1* plants are more susceptible to *P. cucumerina*, which is in line with the previously described role of CERK1 in resistance to other plant pathogenic fungi containing 1,3-β-D-glucans in their cell walls (Wan *et al.*, 2008). In addition to fungi, our data expand the role of CERK1 to the resistance of Arabidopsis to oomycetes, as CERK1 is also required for resistance to the oomycete *H. arabidopsidis* that also has glucan-rich cell walls (Bartnicki-Garcia, 1968; Mélida *et al.*, 2013). Arabidopsis has several hundred potential PRRs, some of them with predicted glycan-binding ectodomains (Wu and Zhou, 2013), that might cooperate with CERK1 in the perception of 1,3-β-D-glucans. Here, we show that ER LRR-RLK, which is required for the resistance of Arabidopsis to *P. cucumerina* and other pathogens, does not play a role in 1,3-β-D-glucan recognition. Though CERK1 is required for immune responses towards different pathogens (e.g. *P. cucumerina*) with glucan-enriched cell walls, *cerk1-2* plants are not as susceptible as other immune-deficient mutants like *agb1-2*, which is impaired in the β subunit of heterotrimeric G protein required for the activation of immune responses modulated by different MAMPs (Liang *et al.*, 2016). Thus, additional fungal cell wall MAMPs to 1,4-β-D-$(GlcNAc)_n$ and 1,3-β-D-$(Glc)_n$ might exist that would not be recognized by the receptor complex harbouring CERK1.

MAMPs are usually slowly evolving components of microbes with crucial biological functions that are not present in the host (Nürnberger *et al.*, 2004). However, this is not completely the case for β-1,3-glucan MAMPs. Plant cells can accumulate callose, a linear β-1,3-glucan with hundreds of glucose units, under specific conditions such as pathogen infection (Stone and Clarke, 1992). Therefore, we cannot exclude the possibility that plant cell walls accumulate β-1,3-glucans as a source of DAMPs able to self-induce PTI responses. This speculation is especially attractive in the case of papillae formation, callose-enriched dome-shaped appositions between the epidermal wall and the plasma membrane synthesized as a plant cell wall reinforcement near the site of pathogen penetration (Huckelhoven, 2007; Albersheim *et al.*, 2011; Chowdhury *et al.*, 2014). Thus, an interesting question that arises is whether Arabidopsis discriminates between self-(DAMP) and non-self-(MAMP) β-1,3-glucans. It has been recently shown that β-1,4-glucan-oligosaccharides (the main component of cellulose) function as DAMPs in Arabidopsis,

© 2017 The Authors

1365313x, 2018, 1, Downloaded from https://onlinelibrary.wiley.com/doi/10.1111/tpj.13755 by Bucle - Universidad De Leon, Wiley Online Library on [13/05/2024]. See the Terms and Conditions (https://onlinelibrary.wiley.com/terms-and-conditions) on Wiley Online Library for rules of use; OA articles are governed by the applicable Creative Commons License

and that the signalling cascade triggered by these DAMPs shares some similarities with chito-oligosaccharides (de Azevedo Souza *et al.*, 2017). In this scenario, ligand availability and proximity to the PRR complexes will be the determining factors, as has been recently proposed (Bücherl *et al.*, 2017). Whether plant callose accumulation and PRR enrichment near infection sites is related to MAMP–DAMP innate immune machinery remains to be elucidated, but it seems quite an attractive strategy for plants to regulate the threshold and amplitude of the plant immune response. Such mechanism would explain the differential kinetics of saturation between chitin and glucans, since small changes in glucan concentration should not activate a PTI response that might result in trade-off effects (Lozano-Durán *et al.*, 2013; Denancé *et al.*, 2013).

EXPERIMENTAL PROCEDURES

Biological material and growth conditions

Plectosphaerella cucumerina (BMM isolate) cells were grown as previously described (Berrocal-Lobo *et al.*, 2002). After 7 days at 28°C mycelia were harvested by filtration on sterile cellulose-free filters (FP Vericel, Pall Corporation, https://www.pall.com/), extensively washed with distilled water to remove the excess of culture medium and stored at −20°C.

All Arabidopsis mutants used in this study were in the Col-0 background, except the *cerk1-3* mutant which was in the Ws-4 background. Details of all mutant lines are provided in Table S4. Arabidopsis plants used for Ca^{2+}_{cyt}, MAPKs and qRT-PCR analyses were grown in 24-well plates (about 10 seedlings per well) under long-day conditions (16 h of light) at 20–22°C in liquid MS medium [0.5 × Murashige and Skoog basal salt medium (Duchefa, https://www.duchefa-biochemie.com/), 0.25% sucrose, 1 mM 2-(*N*-morpholine)-ethanesulphonic acid (MES), pH 5.7].

Carbohydrates

Curdlan, 1,3-β-D-$(Glc)_n$ and 1,4-β-D-$(GlcNAc)_6$ were purchased from Megazyme (https://www.megazyme.com/). The mixture of linear 1,3-β-glucans with a dp ranging from 7 to 16 was also purchased from Megazyme. It was prepared by controlled acid hydrolysis from curdlan from the bacterium *Alcaligenes faecalis* (as well as shorter oligosaccharides), but kept as a batch of high dp instead of further purification to single oligosaccharides. Chitin from crab shells (#C9752) and peptidoglycan from *Bacillus subtilis* (#69554) were obtained from Sigma-Aldrich (http://www.sigmaaldrich.com/). Laminarin was purchased from Thermo Fisher (https://www.thermofisher.com/). 1,4-α-D-$(GalA)_{10\text{-}15}$ (#GAT114) were kindly provided by Elicityl (http://www.elicityl-oligotech.com/).

Preparation and chemical fractionation of cell walls

Frozen fungal cells were disrupted firstly using a kitchen blender cooled with liquid nitrogen followed by homogenization with mortar and pestle until a fine powder was obtained. Powders were treated with 70% (v/v) ethanol twice (1 h and overnight) at 4°C and the supernatants recovered by centrifugation at 1500 ***g*** (10 min). Supernatants were pooled, and the rotaevaporated pellet was the EtOH-I fraction. The mycelial pellet was then treated 70% ethanol twice (1 h each) at 90°C, and the rotaevaporated supernatants were the EtOH-II fractions. The resulting pellet after ethanol treatments was sequentially extracted in order to obtain the purified cell walls and chemical fractions as previously described (Mélida *et al.*, 2013, 2015) (Figure S1).

Carbohydrate analysis

The dried purified cell wall preparations were hydrolysed in the presence of 2 M TFA at 121°C for 3 h. The resulting monosaccharides were converted to alditol acetates (Albersheim *et al.*, 1967). TFA-resistant materials were fully hydrolysed with 72% sulphuric acid at room temperature (25°C) for 3 h followed by 3 h at 100°C after diluting the acid to 1 M (Pettolino *et al.*, 2012). Monosaccharides released by sulphuric acid hydrolysis were converted to alditol acetates as described previously (Blakeney *et al.*, 1983). *Myo*-inositol was used as an internal standard in all cases. Derivatized monosaccharides were separated and analysed by gas chromatography (GC) on a SP-2380 capillary column (30 m × 0.25 mm i.d.; Merck) using a Scion 450-GC system equipped with an EVOQ triple quadrupole (TQ). The temperature programme increased from 165°C to 270°C at a rate of 2°C min^{-1}. Glycosidic linkage analysis was performed as previously described (Mélida *et al.*, 2013). Aminosugars were quantified as previously described (Popolo *et al.*, 1997).

MALDI-TOF MS analyses were performed using a 4800 Plus Proteomics Analyzer MALDI-TOF/TOF mass spectrometer (Applied Biosystems, http://www6.appliedbiosystems.com/).

Aequorin luminescence measurements

Eight-day-old liquid-grown transgenic Arabidopsis seedlings of ecotype Col-0 carrying the calcium reporter aequorin (Col-0^{AEQ}, *bak1-4*^{AEQ} and *cerk1-2*^{AEQ}; Ranf *et al.*, 2011, 2012) were used for cytoplasmic calcium (Ca^{2+}_{cyt}) measurements using the method previously described (Bacete *et al.*, 2017). Negative controls (water) were included in all the experiments. Aequorin luminescence was recorded with a Varioskan Lux Reader (Thermo Scientific, https://www.thermofisher.com/). Thereafter, the total calcium was discharged by adding $CaCl_2$ (1.5 M final concentration) to the wells. The kinetic areas after both treatments were integrated and their values used for the calculations. The dose–response curves and estimated effective dose (EED) values were calculated via non-linear regression considering a variable slope model (four-parameter dose–response curve) using Prism 6 Software (GraphPad Software, https://www.graphpad.com/).

Immunoblot analysis of MAPK activation

Twelve-day-old seedlings grown on liquid MS medium in 24-well plates were treated with *P. cucumerina* fractions, commercial polysaccharides and oligosaccharides for 0, 10, 20 and 30 min, and then harvested in liquid nitrogen. Protein extraction and detection of activated MAPKs using the Phospho-p44/42 MAPK (Erk1/2) (Thr202/Tyr204) antibody (Cell Signaling Technology, https://www.cellsignal.com/) were performed as described (Ranf *et al.*, 2011).

Gene expression analyses

For gene expression analysis (qRT-PCR and RNA sequencing), 12-day-old seedlings grown on liquid MS medium were treated with the MAMPs or water (mock) solutions for 0 and 30 min. Total RNA was purified with the RNeasy Plant Mini Kit (Qiagen, http://www.qiagen.com/) according to the manufacturer's protocol. Quantitative RT-PCR analyses were performed as previously reported (Delgado-Cerezo *et al.*, 2012). *UBC21* (*At5 g25760*) expression was used to normalize the transcript level in each reaction. Oligonucleotides

© 2017 The Authors

1365313x, 2018, 1, Downloaded from https://onlinelibrary.wiley.com/doi/10.1111/tpj.13755 by Bucle - Universidad De Leon, Wiley Online Library on [13/05/2024]. See the Terms and Conditions (https://onlinelibrary.wiley.com/terms-and-conditions) on Wiley Online Library for rules of use; OA articles are governed by the applicable Creative Commons License

used for the detection of gene expression are detailed in Table S5. Analysis of mock-treated seedlings showed no alterations in the expression levels of the marker genes used in this study.

For RNA-seq analyses samples from three biological replicates for each treatment were selected. The quality of these samples was tested for a minimum RNA integrity number (RIN) score of 7 using a 2100 Bioanalyzer (Agilent, http://www.agilent.com/).RNA-seq libraries were prepared from an input of 500 ng total RNA using the TruSeq Stranded mRNA Library Prep Kit (Illumina, https://www.illumina.com/) according to the manufacturer's protocol. Libraries were sequenced with the Illumina HiSeq2500 sequencing platform with single reads of 50 bp. More than 20 million reads were generated per sample. RNA-seq reads were mapped to the Arabidopsis genome (Araport11) using the TopHat 2.1.0 algorithm (Kim *et al.*, 2013). The CuffDiff 2.2.1.3 algorithm (Trapnell *et al.*, 2013) was employed to find significant changes in transcript expression, using geometric normalization to obtain FPKM (fragments per kilobase of transcript per million mapped reads) values for each transcript and gene. A statistical *t*-test was used to compute the significance of the change in FPKM for each gene in the compared conditions. Resulting *P*-values were corrected using Benjamini–Hochberg false discovery rate (FDR) correction for multiple testing. Genes with a FDR-adjusted *P*-value < 0.05 were identified as misregulated for the given comparison. The BiNGO 3.0.3 app (Maere *et al.*, 2005) for Cytoscape 3.5.1 (Smoot *et al.*, 2011) was used to determine which GO categories were statistically overrepresented in the differentially expressed set of genes. Significant enrichments were determined using the hypergeometric test and Benjamini–Hochberg FDR-corrected *P*-values are represented. Cytoscape data represented in Figures 6(b) and S15 are shown in Table S2.

Reactive oxygen species

Three-week-old Arabidopsis plants were used to determine production of ROS after treatments using the luminol assay (Escudero *et al.*, 2017) and a VariosKan Lux luminescence reader (Thermo Scientific). *In vivo* quantification of RbohD promoter-driven luciferase was performed using Arabidopsis transgenic lines *pRbohD::LUC* (Morales *et al.*, 2016). Seven-day-old seedlings grown in liquid MS were transferred to 96-well plates containing 75 μl of distilled water. Then, 25 μl of D-luciferin was added to a final concentration of 0.5 mM and incubated overnight in the dark. Luminescence was recorded with a Varioskan Lux Reader for 240 min after the treatments.

Modelling of AtCERK1-ECD–glycan complex structures

Geometries for AtCERK1-ECD–1,3-β-D-$(Glc)_6$ and AtCERK1-ECD–1,4-β-D-$(GlcNAc)_6$ complexes were first obtained with docking calculations using the crystal structure of AtCERK1-ECD (PDB code 4EBZ). Hexamer crystal structures: 1,3-β-D-$(Glc)_6$, PDB code 1W9W; 1,4-β-D-$(GlcNAc)_6$, PDB code 2PI8. Docking calculations were performed with AutoDock Vina (Trott and Olson, 2010). Cubic spatial grids of side 25 Å centred at 3D coordinates that correspond to a central atom in chitotetraose (O3 atom of the NAG814 subunit) present in the 4EBZ crystal structure were used for a pose search in Vina calculations. In all cases the best docking geometry was selected as the initial structure for subsequent modelling. The K_d dissociation constants for docked complexes were then estimated from ΔG_{aff} values as $K_d = \exp(-\Delta G_{aff}/RT)$ at $T = 298.15$ K.

Each AtCERK1-ECD–glycan docking complex was then immersed in a solvation box with 12 Å padding in the three dimensions using the TIP3P water model (Jorgensen *et al.*, 1983) adding Na^+ and Cl^- ions to neutralize the system while setting the salt concentration to 0.150 M with VMD 1.9.3 (Humphrey *et al.* 1996). The geometries of the molecular systems thus constructed were optimized at 5000 steps of a conjugate gradient algorithm with NAMD 2.10 (Phillips *et al.*, 2005) in molecular mechanics calculations using the CHARMM force field.

Energy terms contributing to protein–ligand binding free energies ΔG_{bind} were computed using the molecular mechanics (MM) with Poisson–Boltzmann (PB) and surface area (SA) solvation MM/PBSA approach applied to AtCERK1-ECD–glycan CHARMM-optimized geometries (see Table S1 for details).

Pathogenicity assays

Inoculations with *P. cucumerina* BMM isolate were performed by spraying 18-day-old plants ($n > 10$) grown on soil as described in Delgado-Cerezo *et al.* (2012) with a suspension of 4×10^6 spores ml^{-1} of the fungus. Disease progression in the inoculated plants was estimated by means of qPCR as previously described (Delgado-Cerezo *et al.*, 2012). *Hyaloperonospora arabidopsidis* isolate Noco2 (2×10^4 spores ml^{-1}) was spray-inoculated onto 2-week-old plants ($n > 20$) and spore numbers determined at 7 dpi (Llorente *et al.*, 2005). *Hyaloperonospora arabidopsidis* hyphae were detected by trypan blue staining of leaves at 7 dpi (Llorente *et al.*, 2005). Triplicates were done for all the pathogenicity experiments.

ACCESSION NUMBERS

RNA-seq read data have been submitted to the NCBI Sequence Read Archive (SRA) under accession SRP111065.

ACKNOWLEDGEMENTS

We thank Dr D. Scheel (Leibniz Institute of Plant Biochemistry, Germany), Dr C. Zipfel (Sainsbury Laboratory, UK), Dr T. Nürnberger and Dr Andrea Gust (University of Tübingen, Germany), Dr M. Knight (Durham University, UK) and Dr J. E. Parker (Max Planck Institute for Plant Breeding Research, Cologne) for providing biological materials. We thank the Megazyme Technical Support Team and Dr Benoit Darblade (Elicytil, France) for providing quality control analyses of the MAMPs/DAMPs used in this article. The MALDI-TOF MS analyses were performed in the Proteomics Unit of Complutense University of Madrid that belongs to ProteoRed (PRB2-ISCIII supported by grant PT13/0001). This work was supported by Spanish Ministry of Economy and Competitiveness (MINECO) grants BIO2015-64077-R and BIO2012-32910 to AM and BIO2013-41403-R to LFP. HM was funded by an IEF grant (SignWALLNg-624721) from the European Union and LB was recipient of a FPI fellowship (BES-2013-065010) from MINECO.

CONFLICT OF INTEREST

All authors confirm that there are no conflicts of interest to declare.

SUPPORTING INFORMATION

Additional Supporting Information may be found in the online version of this article.

Figure S1. Preparation and fractionation of *Plectosphaerella cucumerina* cell wall carbohydrates.

Figure S2. Glycosidic linkage analysis (mol%) of *Plectosphaerella cucumerina* mycelium and spore cell walls.

Figure S3. Quantitative RT-PCR analyses of microbe-associated molecular pattern (MAMP)-inducible genes in Arabidopsis seedlings of the indicated genotypes treated with cell wall MAMPs

Figure S4. Matrix-assisted laser desorption ionization-time of flight mass spectra of *Plectosphaerella cucumerina* mycelial ASF-II.

© 2017 The Authors

1365313x, 2018, 1, Downloaded from https://onlinelibrary.wiley.com/doi/10.1111/tpj.13755 by Bucle - Universidad De Leon, Wiley Online Library on [13/05/2024]. See the Terms and Conditions (https://onlinelibrary.wiley.com/terms-and-conditions) on Wiley Online Library for rules of use; OA articles are governed by the applicable Creative Commons License

Figure S5. Quantitative RT-PCR analyses of of microbe-associated molecular pattern (MAMP)-inducible genes in Arabidopsis seedlings of the indicated genotypes treated with MAMPs.

Figure S6. Mitogen-activated protein kinase activation and qRT-PCR analyses of defence and microbe-associated molecular pattern-induced genes in Arabidopsis *cerk1-3* seedlings.

Figure S7. Production of reactive oxygen species.

Figure S8. Purity analyses of 1,3-β-D-$(Glc)_6$ samples.

Figure S9. Mitogen-activated protein kinase activation in 12-day-old Arabidopsis seedlings of the indicated genotypes.

Figure S10. Elevations of cytoplasmic calcium concentrations over time in Arabidopsis Col-0^{AEQ}, *cerk1-2*^{AEQ} and *bak1-4*^{AEQ} seedlings.

Figure S11. Matrix-assisted laser desorption ionization-time of flight mass spectra of 1,3-β-D-glucans with a high degree of polymerization.

Figure S12. Activation of pattern-triggered immunity responses by 1,3-β-D-$(Glc)_{7–16}$.

Figure S13. Elevations of cytoplasmic calcium concentrations over time in Arabidopsis Col-0^{AEQ} and *cerk1-2*^{AEQ} seedlings upon treatment with 0.25 mg ml^{-1} of glucan polysaccharides.

Figure S14. Dose dependence of the total cytoplasmic calcium elevations in Arabidopsis Col-0^{AEQ} seedlings upon treatments with increasing concentrations of flg22.

Figure S15. Gene Ontology biological process-term enrichment network of the misregulated genes in *cerk1-2* upon treatment.

Figure S16. Mitogen-activated protein kinase activation in 12-day-old Arabidopsis seedlings of the indicated genotypes upon application of *Plectosphaerella cucumerina* ASF-II.

Figure S17. Trypan blue staining of leaves the indicated genotypes at 7 days post-inoculation with *Hyaloperonospora arabidopsidis* Noco2.

Table S1. AtCERK1-ECD–glycan energies.

Table S2. Differentially expressed genes in Col-0 and cerk1-2 seedlings treated during 30 min with 250 μM 1,3-β-D-$(Glc)_6$.

Table S3. Gene Ontology categories statistically overrepresented in the differentially expressed set of genes.

Table S4. Arabidopsis genotypes used in this study.

Table S5. Primers used for gene expression analyses.

REFERENCES

Adams, E.L., Rice, P.J., Graves, B. *et al.* (2008) Differential high-affinity interaction of dectin-1 with natural or synthetic glucans is dependent upon primary structure and is influenced by polymer chain length and side-chain branching. *J. Pharmacol. Exp. Ther.* **325**, 115–123.

Albersheim, P. and Valent, B.S. (1978) Host-pathogen interactions in plants. Plants, when exposed to oligosaccharides of fungal origin, defend themselves by accumulating antibiotics. *J. Cell Biol.* **78**, 627–643.

Albersheim, P., Nevins, D.J., English, P.D. and Karr, A. (1967) A method for the analysis of sugars in plant cell-wall polysaccharides by gas-liquid chromatography. *Carbohydr. Res.* **5**, 340–345.

Albersheim, P., Darvill, A., Roberts, K., Sederoff, R. and Staehelin, A. (2011) *Cell Walls and Plant-Microbe Interactions*. New York, NY: Garland Science, Taylor & Francis.

Albert, I., Böhm, H., Albert, M. *et al.* (2015) An RLP23-SOBIR1-BAK1 complex mediates NLP-triggered immunity. *Nat. Plants*, **1**, 15140.

Anderson, A.J. (1978) The isolation from three species of Colletotrichum of glucan containing polysaccharides that elicit a defense response in bean (Phaseolus vulgaris). *Phytopathol.* **68**, 189–194.

Anderson, A.J. (1980) Studies on the structure and elicitor activity of fungal glucans. *Can. J. Bot.* **58**, 2343–2348.

Ariizumi, K., Shen, G.L., Shikano, S., Xu, S., Ritter, R., Kumamoto, T., Edelbaum, D., Morita, A., Bergstrasser, P.R. and Takashima, A. (2000) Identification of a novel, dendritic cell-associated molecule, dectin-1, by subtractive cDNA cloning. *J. Biol. Chem.* **275**, 20157–20167.

Ayers, A.R., Ebel, J., Valent, B. and Albersheim, P. (1976) Host-pathogen interactions: x. fractionation and biological activity of an elicitor isolated from the mycelial walls of phytophthora megasperma var. sojae. *Plant Physiol.* **57**, 760–765.

de Azevedo Souza, C., Li, S., Lin, A.Z., Boutrot, F., Grossmann, G., Zipfel, C. and Somerville, S. (2017) Cellulose-derived oligomers act as damage-associated molecular patterns and trigger defense-like responses. *Plant Physiol.* **173**, 2383–2398.

Bacete, L., Mélida, H., Pattathil, S., Hahn, M.G., Molina, A. and Miedes, E. (2017) Characterization of plant cell wall damage-associated molecular patterns regulating immune responses. *Methods Mol. Biol.* **1578**, 13–23.

Bartnicki-Garcia, S. (1968) Cell wall chemistry, morphogenesis, and taxonomy of fungi. *Annu. Rev. Microbiol.* **22**, 87–108.

Bauer, Z., Gómez-Gómez, L., Boller, T. and Felix, G. (2001) Sensitivity of different ecotypes and mutants of Arabidopsis thaliana toward the bacterial elicitor flagellin correlates with the presence of receptor-binding sites. *J. Biol. Chem.* **276**, 45669–45676.

Berrocal-Lobo, M., Molina, A. and Solano, R. (2002) Constitutive expression of ETHYLENE-RESPONSE-FACTOR1 in Arabidopsis confers resistance to several necrotrophic fungi. *Plant J.* **29**, 23–32.

Bigeard, J., Colcombet, J. and Hirt, H. (2015) Signaling mechanisms in pattern-triggered immunity (PTI). *Mol. Plant*, **8**, 521–539.

Blakeney, A.B., Harris, P.J., Henry, R.J. and Stone, B.A. (1983) A simple and rapid preparation of alditol acetates for monosaccharide analysis. *Carbohydr. Res.* **113**, 291–299.

Brown, G.D. and Gordon, S. (2003) Fungal β-glucans and mammalian immunity. *Immunity*, **19**, 311–315.

Brown, G.D., Herre, J., Williams, D.L., Willment, J.A., Marshall, A.S. and Gordon, S. (2003) Dectin-1 mediates the biological effects of β-glucans. *J. Exp. Med.* **197**, 1119–1124.

Bücherl, C.A., Jarsch, I.K., Schudoma, C., Segonzac, C., Mbengue, M., Robatzek, S., MacLean, D., Ott, T. and Zipfel, C. (2017) Plant immune and growth receptors share common signalling components but localise to distinct plasma membrane nanodomains. *eLife*, **6**, e25114.

Cantu, D., Greve, L.C., Labavitch, J.M. and Powell, A.L.T. (2009) Characterization of the cell wall of the ubiquitous plant pathogen Botrytis cinerea. *Mycol. Res.* **113**, 1396–1403.

Cao, Y., Liang, Y., Tanaka, K., Nguyen, C.T., Jedrzejczak, R.P., Joachimiak, A. and Stacey, G. (2014) The kinase LYK5 is a major chitin receptor in Arabidopsis and forms a chitin-induced complex with related kinase CERK1. *eLife*, **3**, e03766.

Chinchilla, D., Bauer, Z., Regenass, M., Boller, T. and Felix, G. (2006) The Arabidopsis receptor kinase FLS2 binds flg22 and determines the specificity of flagellin perception. *Plant Cell*, **18**, 465–476.

Chowdhury, J., Henderson, M., Schweizer, P., Burton, R.A., Fincher, G.B. and Little, A. (2014) Differential accumulation of callose, arabinoxylan and cellulose in nonpenetrated versus penetrated papillae on leaves of barley infected with Blumeria graminis f. sp. hordei. *New Phytol.* **204**, 650–660.

Czop, J.K. (1986) The role of β -glucan receptors on blood and tissue leukocytes in phagocytosis and metabolic activation. *Pathol. Immunopathol. Res.* **5**, 286–296.

Delgado-Cerezo, M., Sánchez-Rodríguez, C., Escudero, V. *et al.* (2012) Arabidopsis heterotrimeric G-protein regulates cell wall defense and resistance to necrotrophic fungi. *Mol. Plant*, **5**, 98–114.

Denancé, N., Sánchez-Vallet, A., Goffner, D. and Molina, A. (2013) Disease resistance or growth: the role of plant hormones in balancing immune responses and fitness costs. *Front. Plant Sci.* **4**, 155.

Ebel, J., Ayers, A.R. and Albersheim, P. (1976) Host-Pathogen Interactions: XII. Response of Suspension-cultured Soybean Cells to the Elicitor Isolated from Phytophthora megasperma var. sojae, a Fungal Pathogen of Soybeans. *Plant Physiol.* **57**, 775–779.

Erwig, J., Ghareeb, H., Kopischke, M., Hacke, R., Matei, A., Petutschnig, E. and Lipka, V. (2017) Chitin-induced and CHITIN ELICITOR RECEPTOR KINASE1 (CERK1) phosphorylation-dependent endocytosis of Arabidopsis thaliana LYSIN MOTIF-CONTAINING RECEPTOR-LIKE KINASE5 (LYK5). *New Phytol.* **215**, 382–396.

Escudero, V., Jordá, L., Sopeña-Torres, S. *et al.* (2017) Alteration of cell wall xylan acetylation trigger defense responses that counterbalance the

© 2017 The Authors

1365313x, 2018, 1, Downloaded from https://onlinelibrary.wiley.com/doi/10.1111/tpj.13755 by Bucle - Universidad De Leon, Wiley Online Library on [13/05/2024]. See the Terms and Conditions (https://onlinelibrary.wiley.com/terms-and-conditions) on Wiley Online Library for rules of use; OA articles are governed by the applicable Creative Commons License

immune deficiencies of plants impaired in the β subunit of the heterotrimeric G protein. *Plant J.* **92**, 386–399, in press.

Fesel, P.H. and Zuccaro, A. (2016) β-glucan: crucial component of the fungal cell wall and elusive MAMP in plants. *Fungal Genet. Biol.* **90**, 53–60.

Fisher, M.C., Henk, D.A., Briggs, C.J., Brownstein, J.S., Madoff, L.C., McCraw, S.L. and Gurr, S.J. (2012) Emerging fungal threats to animal, plant and ecosystem health. *Nature*, **484**, 186–194.

Geoghegan, I., Steinberg, G. and Gurr, S. (2017) The role of the fungal cell wall in the infection of plants. *Trends Microbiol.* **5**, 405–408. [Epub ahead of print].

Gómez-Gómez, L. and Boller, T. (2000) FLS2: an LRR receptor-like kinase involved in the perception of the bacterial elicitor flagellin in Arabidopsis. *Mol. Cell*, **5**, 1003–1011.

Gómez-Gómez, L., Felix, G. and Boller, T. (1999) A single locus determines sensitivity to bacterial flagellin in Arabidopsis thaliana. *Plant J.* **18**, 277–284.

Heidrich, K., Wirthmueller, L., Tasset, C., Pouzet, C., Deslandes, L. and Parker, J.E. (2011) Arabidopsis EDS1 connects pathogen effector recognition to cell compartment-specific immune responses. *Science*, **334**, 1401–1404.

Hernández-Blanco, C., Feng, D.X., Hu, J. *et al.* (2007) Impairment of cellulose synthases required for Arabidopsis secondary cell wall formation enhances disease resistance. *Plant Cell*, **19**, 890–903.

Huckelhoven, R. (2007) Cell wall–associated mechanisms of disease resistance and susceptibility. *Annu. Rev. Phytopathol.* **45**, 101–127.

Humphrey, W., Dalke, A. and Schulten, K. (1996) VMD – visual molecular dynamics. *J. Mol. Graph.* **14**, 33–38.

Jordá, L., Sopeña-Torres, S., Escudero, V., Nuñez-Corcuera, B., Delgado-Cerezo, M., Torii, K.U. and Molina, A. (2016) ERECTA and BAK1 Receptor Like Kinases Interact to Regulate Immune Responses in Arabidopsis. *Front. Plant Sci.* **7**, 897.

Jorgensen, W., Chandrasekhar, J., Madura, J., Impey, R.W. and Klein, M. (1983) Comparison of simple potential functions for simulating liquid water. *J. Chem. Phys.* **79**, 926–933.

Kaku, H., Nishizawa, Y., Ishii-Minami, N., Akimoto-Tomiyama, C., Dohmae, N., Takio, K., Minami, E. and Shibuya, N. (2006) Plant cells recognize chitin fragments for defense signalling through a plasma membrane receptor. *Proc. Natl Acad. Sci. USA*, **103**, 11086–11091.

Kemmerling, B., Schwedt, A., Rodriguez, P. *et al.* (2007) The BRI1-associated kinase 1, BAK1, has a brassinolide-independent role in plant cell-death control. *Curr. Biol.* **17**, 1116–1122.

Kim, D., Pertea, G., Trapnell, C., Pimentel, H., Kelley, R. and Salzberg, S.L. (2013) TopHat2: accurate alignment of transcriptomes in the presence of insertions, deletions and gene fusions. *Genome Biol.* **14**, R36.

Klarzynski, O., Plesse, B., Joubert, J.M., Yvin, J.C., Kopp, M., Kloareg, B. and Fritig, B. (2000) Linear beta-1,3 glucans are elicitors of defense responses in tobacco. *Plant Physiol.* **124**, 1027–1038.

Latgé, J.P. (2017) Immune evasion: face changing in the fungal opera. *Nat. Microbiol.* **2**, 16266.

Latgé, J.P. and Calderone, R. (2006) The fungal cell wall. In *The Mycota I. Growth, Differentiation and Sexuality* (Kües, U. and Fischer, R. eds). Heidelberg, Germany: Springer Berlin, pp. 73–104.

Leal, J.A., Prieto, A., Bernabé, M. and Hawksworth, D.L. (2010) An assessment of fungal wall heteromannans as a phylogenetically informative character in ascomycetes. *FEMS Microbiol. Rev.* **34**, 986–1014.

Li, J. (2010) Multi-tasking of somatic embryogenesis receptor-like protein kinases. *Curr. Opin. Plant Biol.* **13**, 509–514.

Liang, X., Ding, P., Lian, K. *et al.* (2016) Arabidopsis heterotrimeric G proteins regulate immunity by directly coupling to the FLS2 receptor. *eLife* **5**, e13568.

Liu, T., Liu, Z., Song, C. *et al.* (2012) Chitin-induced dimerization activates a plant immune receptor. *Science*, **336**, 1160–1164.

Liu, S., Wang, J., Han, Z., Gong, X., Zhang, H. and Chai, J. (2016) Molecular mechanism for fungal cell wall recognition by rice chitin receptor OsCEBiP. *Structure*, **24**, 1192–1200.

Llorente, F., Alonso-Blanco, C., Sánchez-Rodríguez, C., Jordá, L. and Molina, A. (2005) ERECTA receptor-like kinase and heterotrimeric G protein from Arabidopsis are required for resistance to the necrotrophic fungus Plectosphaerella cucumerina. *Plant J.* **43**, 165–180.

Lozano-Durán, R., Macho, A.P., Boutrot, F., Segonzac, C., Somssich, I.E. and Zipfel, C. (2013) The transcriptional regulator BZR1 mediates trade-off between plant innate immunity and growth. *eLife* **2**, e00983.

Maere, S., Heymans, K. and Kuiper, M. (2005) BiNGO: a Cytoscape plugin to assess overrepresentation of Gene Ontology categories in biological networks. *Bioinformatics*, **21**, 3448–3449.

Mélida, H., Sandoval-Sierra, J.V., Diéguez-Uribeondo, J. and Bulone, V. (2013) Analyses of extracellular carbohydrates in oomycetes unveil the existence of three different cell wall types. *Eukaryot. Cell*, **12**, 194–203.

Mélida, H., Sain, D., Stajich, J.E. and Bulone, V. (2015) Deciphering the uniqueness of Mucoromycotina cell walls by combining biochemical and phylogenomic approaches. *Environ. Microbiol.* **17**, 1649–1662.

Ménard, R., Alban, S., de Ruffray, P., Jamois, F., Franz, G., Fritig, B., Yvin, J.C. and Kauffmann, S. (2004) & #x03B2;-1,3 glucan sulfate, but not & #x03B2;-1,3 glucan, induces the salicylic acid signaling pathway in tobacco and Arabidopsis. *Plant Cell*, **16**, 3020–3032.

Miya, A., Albert, P., Shinya, T., Desaki, Y., Ichimura, K., Shirasu, K., Narusaka, Y., Kawakami, N., Kaku, H. and Shibuya, N. (2007) CERK1, a LysM receptor kinase, is essential for chitin elicitor signaling in Arabidopsis. *Proc. Natl Acad. Sci. USA*, **104**, 19613–19618.

Morales, J., Kadota, Y., Zipfel, C., Molina, A. and Torres, M.A. (2016) The Arabidopsis NADPH oxidases RbohD and RbohF display differential expression patterns and contributions during plant immunity. *J. Exp. Bot.* **67**, 1663–1676.

Nothnagel, E.A., McNeil, M., Albersheim, P. and Dell, A. (1983) Host-Pathogen Interactions: XXII. A galacturonic acid oligosaccharide from plant cell walls elicits phytoalexins. *Plant Physiol.* **71**, 916–926.

Nürnberger, T., Brunner, F., Kemmerling, B. and Piater, L. (2004) Innate immunity in plants and animals: striking similarities and obvious differences. *Immunol. Rev.* **198**, 249–266.

Palma, A.S., Feizi, T., Zhang, Y. *et al.* (2006) Ligands for the β-glucan receptor, Dectin-1, assigned using "designer" microarrays of oligosaccharide probes (neoglycolipids) generated from glucan polysaccharides. *J. Biol. Chem.* **281**, 5771–5779.

Pettolino, F.A., Walsh, C., Fincher, G.B. and Bacic, A. (2012) Determining the polysaccharide composition of plant cell walls. *Nat. Protoc.* **7**, 1590–1607.

Phillips, J.C., Braun, R., Wang, W., Gumbart, J., Tajkhorshid, E., Villa, E., Chipot, C., Skeel, R.D., Kalé, L. and Schulten, K. (2005) Scalable molecular dynamics with NAMD. *J. Comput. Chem.* **26**, 1781–1802.

Popolo, L., Gilardelli, D., Bonfante, P. and Vai, M. (1997) Increase in chitin as an essential response to defects in assembly of cell wall polymers in the ggp1delta mutant of Saccharomyces cerevisiae. *J. Bacteriol.* **179**, 463–469.

Ramos, B., Gonzalez-Melendi, P., Sánchez-Vallet, A., Sánchez-Rodriguez, C., López, G. and Molina, A. (2013) Functional genomics tools to decipher the pathogenicity mechanisms of the necrotrophic fungus Plectosphaerella cucumerina in Arabidopsis thaliana. *Mol. Plant. Pathol.* **14**, 44–57.

Ranf, S., Eschen-Lippold, L., Pecher, P., Lee, J. and Scheel, D. (2011) Interplay between calcium signalling and early signalling elements during defence responses to microbe- or damage-associated molecular patterns. *Plant J.* **68**, 100–113.

Ranf, S., Grimmer, J., Pöschl, Y., Pecher, P., Chinchilla, D., Scheel, D. and Lee, J. (2012) Defense-related calcium signaling mutants uncovered via a quantitative high-throughput screen in Arabidopsis thaliana. *Mol. Plant*, **5**, 115–130.

Rovenich, H., Zuccaro, A. and Thomma, B.P. (2016) Convergent evolution of filamentous microbes towards evasion of glycan-triggered immunity. *New Phytol.* **212**, 896–901.

Samalova, M., Mélida, H., Vilaplana, F., Bulone, V., Soanes, D.M., Talbot, N.J. and Gurr, S.J. (2017) The β-1,3-glucanosyltransferases (Gels) affect the structure of the rice blast fungal cell wall during appressorium-mediated plant infection. *Cell. Microbiol.* **19**, e12659.

Seybold, H., Trempel, F., Ranf, S., Scheel, D., Romeis, T. and Lee, J. (2014) Ca^{2+} signalling in plant immune response: from pattern recognition receptors to Ca^{2+} decoding mechanisms. *New Phytol.* **204**, 782–790.

Sharp, J.K., McNeil, M. and Albersheim, P. (1984) The primary structures of one elicitor-active and seven elicitor-inactive hexa(β-D-glucopyranosyl)-D-glucitols isolated from the mycelial walls of Phytophthora megasperma f. sp. glycinea. *J. Biol. Chem.* **259**, 11321–11336.

Smoot, M.E., Ono, K., Ruscheinski, J., Wang, P.L. and Ideker, T. (2011) Cytoscape 2.8: new features for data integration and network visualization. *Bioinformatics*, **27**, 431–432.

© 2017 The Authors

1365313x, 2018, 1, Downloaded from https://onlinelibrary.wiley.com/doi/10.1111/tpj.13755 by Bucle - Universidad De Leon, Wiley Online Library on [13/05/2024]. See the Terms and Conditions (https://onlinelibrary.wiley.com/terms-and-conditions) on Wiley Online Library for rules of use; OA articles are governed by the applicable Creative Commons License

Stone, B.A. and Clarke, A.E. (1992) *Chemistry and biology of (1→3)-β-glucans*. Victoria, Australia: La Trobe University Press, La Trobe University.

Trapnell, C., Hendrickson, D.G., Sauvageau, M., Goff, L., Rinn, J.L. and Pachter, L. (2013) Differential analysis of gene regulation at transcript resolution with RNA-seq. *Nat. Biotechnol.* **31**, 46–53.

Trott, O. and Olson, A.J. (2010) AutoDock Vina: improving the speed and accuracy of docking with a new scoring function, efficient optimization, and multithreading. *J. Comput. Chem.* **25**, 1605–1612.

Wan, J., Zhang, X.C., Neece, D., Ramonell, K.M., Clough, S., Kim, S.Y., Stacey, M.G. and Stacey, G. (2008) A LysM receptor-like kinase plays a critical role in chitin signaling and fungal resistance in Arabidopsis. *Plant Cell*, **20**, 471–481.

Wawra, S., Fesel, P., Widmer, H. *et al.* (2016) The fungal-specific β-glucan-binding lectin FGB1 alters cell-wall composition and suppresses glucan-triggered immunity in plants. *Nat. Commun.* **27**, 13188.

Williams, D.L. (1997) Overview of (1,3)-β-D-glucan immunobiology. *Mediators Inflamm.* **6**, 247–250.

Willmann, R., Lajunen, H.M., Erbs, G. *et al.* (2011) Arabidopsis lysin-motif proteins LYM1 LYM3 CERK1 mediate bacterial peptidoglycan sensing and immunity to bacterial infection. *Proc. Natl Acad. Sci. USA*, **108**, 19824–19829.

Wu, Y. and Zhou, J.M. (2013) Receptor-like kinases in plant innate immunity. *J. Integr. Plant Biol.* **55**, 1271–1286.

Yamaguchi, T., Yamada, A., Hong, N., Ogawa, T., Ishii, T. and Shibuya, N. (2000) Differences in the recognition of glucan elicitor signals between rice and soybean: beta-glucan fragments from the rice blast disease fungus Pyricularia oryzae that elicit phytoalexin biosynthesis in suspension-cultured rice cells. *Plant Cell*, **12**, 817–826.

Zhang, W., Fraiture, M., Kolb, D., Löffelhardt, B., Desaki, Y., Boutrot, F.F., Tör, M., Zipfel, C., Gust, A.A. and Brunner, F. (2013) Arabidopsis receptor-like protein30 and receptor-like kinase suppressor of BIR1-1/EVERSHED mediate innate immunity to necrotrophic fungi. *Plant Cell*, **25**, 4227–4241.

© 2017 The Authors

1365313x, 2018, 1, Downloaded from https://onlinelibrary.wiley.com/doi/10.1111/tpj.13755 by Bucle - Universidad De Leon, Wiley Online Library on [13/05/2024]. See the Terms and Conditions (https://onlinelibrary.wiley.com/terms-and-conditions) on Wiley Online Library for rules of use; OA articles are governed by the applicable Creative Commons License